Piecewise Linear Approximation of Quasiconformal Mappings by Certain Linear Systems

Dissertation

Hirokazu Shimauchi

Division of Mathematics
Graduate School of Information Sciences
Tohoku University

Contents

1 Introduction **1**

2 Preliminaries **5**

2.1 Quasiconformal mappings 5

2.1.1 Quasiconformality 5

2.1.2 Measurable Riemann mapping theorem 6

2.1.3 Composition and distortion lemmas for quasiconformal mappings 7

2.1.4 Normal families of the quasiconformal mappings 8

2.1.5 Conformal module 9

2.1.6 Affine linear quasiconformal mappings 11

2.2 Simplicial approximation and least squares 12

2.2.1 Triangulation and piecewise linear mapping 13

2.2.2 Secant mapping and least squares 15

3 Algorithm for quasiconformal mappings **17**

3.1 Setting 17

3.2 Discrete Beltrami equation 17

3.2.1 Logarithmic coordinates 18

3.2.2 Domain of definition and triangulation 18

3.2.3 Beltrami coefficients in the logarithmic coordinates . . 20

3.2.4 Triangle equations 21

3.2.5 Boundary equations 22

3.2.6 Normalization 23

3.3 Associated linear system 24

3.4 Approximation of the solution 24
3.4.1 Least squares solution 24
3.4.2 Exponential mapping 26

4 Convergence **27**
4.1 Convergence of the approximations 27

5 Numerical experiments **37**
5.1 Comparison with true solution 37
5.1.1 Constant Beltrami coefficient 37
5.1.2 Radial quasiconformal mappings 41
5.1.3 Sectorial quasiconformal mappings 42
5.2 Trivial Beltrami coefficients 42
5.3 Comparison with Daripa's method 45
5.4 Computational cost 47
5.5 Future tasks 48

Appendix **49**

Notation **55**

Acknowledgements **57**

Chapter 1

Introduction

Quasiconformal mappings are a natural generalization of conformal mappings. There are several definitions for quasiconformality, which are based on generalizations of certain properties of conformal mappings (we will introduce a definition of quasiconformal mappings in Chapter 2). Further various theorems for analytic functions are valid for quasiconformal mappings at least in modified form (see [20] for details). Quasiconformal mappings were introduced by H. Grötzsch in 1928. Afterwards, this theory was developed further by many mathematicians in this field. Applications can be found in different areas of mathematics, such as complex dynamical systems (see e.g. [1], [28]), Teichmüller space (see e.g. [1], [13], [17]) and so on.

Recently, some numerical methods for quasiconformal mappings with practical applications were presented in different scientific area. A finite difference method for the quasiconformal mapping was presented in Mastin-Tompson [27]. This method is applied to the finite grid generation [27]. Weisel [38] proposed a finite element based method and applied it to the determination of the modulus of quadrilaterals. A method based on the proof of the existence theorem for quasiconformal mapping by Ahlfors-Bers [2], was presented in Daripa [6]. This method is an iterative scheme which uses singular integral transforms. Their work includes a refinement of the technique of evaluation of the singular integrals, which is of interest in itself. A related approach involving the singular integrals was developed by P. Daripa

and D. Mashat [8, 7], and refined by D. Gaidashev and D. Khmelev [12]. Zh.-X. He [15] and B. Williams [39] proposed alternative methods which are based on circle packings. A circle packing, is considered to be a collection of closed disks with disjoint interiors and prescribed tangencies, induces a simplicial complex between the domains. The induced sequence of piecewise linear mappings by circle packings, convergence to the Riemann mapping. The convergence was suggested by W. Thurston for a geometric proof of the Riemann mapping theorem, and the proof has been worked out by Rodin-Sullivan [33]. A method based on the Beltrami holomorphic flow is presented in Lui et al. [23], and applied to the medical image processing and data compression. Lui et al. [24] described yet another method, which reduces the question of solving the Beltrami equation to that of a linear system on the underlying mesh. Their method, focused on obtaining Teichmüller mappings of prescribed domains, is applied to problems of face recognition and brain mapping.

In this thesis, we propose a numerical method for quasiconformal mappings of the unit disk. Our method considers a well known lemma for quasiconformal mappings, the so called good approximation lemma (see Lemma J). The unit disk is triangulated in a simple way and quasiconformal mappings are approximated by piecewise linear mappings. The images of the vertices of the triangles are defined by an overdetermined system of linear equations. Further the sequence of the approximation converges to the true solution in some certain cases, such as our main theorem (Theorem 4.1.1).

In Chapter 2, we prepare some definitions, notations and known results which we will use in the latter part of this work. First we give a definition of the quasiconformal mapping, and introduce some basic properties of quasiconformal mappings. In particular, we will introduce the Beltrami coefficient and the Beltrami equation, which is deeply related to the quasiconformal mapping. In the following steps, we define the triangulation of the unit disk in our setting, and then define the secant map and piecewise linear space for the triangulation. A proof for a lemma for piecewise linear mappings in this special setting is presented. Further we define the least squares solution for an over determined linear systems.

The detailed setting of the problem is formulated in Chapter 3, where we also present our algorithm. First we will define the vertices of the triangulation, and construct an overdetermined linear system by these vertices and the Beltrami coefficient. In the end of this chapter, we present our approximation for a quasiconformal mapping.

In Chapter 4, the main theorem for the convergence of the approximations (Theorem 4.1.1) is stated. Our proof is stated for the case that the Beltrami coefficients are in $C^1(\mathbb{D})$, i.e. the Beltrami coefficient is continuously differentiable on the unit disk (we conjecture that the condition is overly restrictive by the numerical experiments).

Finally several numerical experiments are presented in Chapter 5. First we compare the results which were produced by our algorithm, with the exact formulas for the quasiconformal mappings under consideration. Then we compare our method with the method by Daripa. Furthermore several experiments for various Beltrami coefficients are presented. The computational cost of our method is estimated. At last we will conclude this work with a short summary of our studies. This thesis is based on the joint work with Professor R. Michael Porter [32].

Chapter 2

Preliminaries

In this chapter, we prepare some definitions, notations and basic facts which we will use. The contents come from the theory of quasiconformal mappings, simplicial approximation and Least squares method.

2.1 Quasiconformal mappings

2.1.1 Quasiconformality

We will define the quasiconformal mapping in the plane. There are some definitions for the quasiconformality. For convenience, we use the analytic definition. See e.g. [1] and [20] for other definitions and the proof for the equivalence.

Definition A ([1, p. 17]). *Let $K > 1$ and D, D' be the domains in the complex plane $\mathbb{C}$. An sense preserving homeomorphism $f : D \to D'$ is a K-quasiconformal mapping if f satisfies the following:*

1. *For any closed rectangle $R := \{x + iy \,|\, a \leq x \leq b, c \leq y \leq d\}$, f is absolutely continuous on almost every horizontal and vertical line in R.*

2. *The dilatation condition*

$$|f_{\overline{z}}(z)| \leq \frac{K-1}{K+1}|f_z(z)| \tag{2.1.1}$$

holds almost everywhere in D, where $f_z = (f_x - if_y)/2$, $f_{\overline{z}} = (f_x + if_y)/2$.

It follows from the definition that the quasiconformal mapping $f : D \to D'$ has partial derivatives $f_z := (f_x - if_y)/2$, $f_{\overline{z}} := (f_x + if_y)/2$ almost everywhere in D. Further f is differentiable a.e. in D, i.e. the linear approximation

$$f(z) - f(z_0) = f_z(z_0)(z - z_0) + f_{\overline{z}}(z_0)(\overline{z} - \overline{z_0}) + o(|z - z_0|)$$

holds a.e. in D (see e.g. [1, p. 17]). The Beltrami coefficients can be defined as

$$\mu_f(z) := \frac{f_z(z)}{f_{\overline{z}}(z)} \tag{2.1.2}$$

a.e. in D for a quasiconformal mapping f, which is a measure of non-conformality (see e.g. [1, p. 7]). In particular, f is conformal at a point $z_0 \in D$ if $\mu_f(z_0) = 0$.

2.1.2 Measurable Riemann mapping theorem

We consider the following Beltrami equation

$$f_{\overline{z}} = \mu f_z \tag{2.1.3}$$

with a prescribed Beltrami coefficient μ. The existence theorem for the solution of the Beltrami equation is called Measurable Riemann mapping theorem (see e.g. [1, p. 57] and [20, p. 194]). The first proof of the existence theorem for the measurable Beltrami coefficients was given by Morrey. Alternative proofs were given by Ahlfors-Bers, Bers-Nirenberg and Bojarskii (see [2] for the historical remark).

Theorem B (Measurable Riemann mapping theorem (see e.g. [1, p. 57] and [20, p. 194]))**.** *Let μ be a measurable function in $\mathbb{C}$ with $\|\mu\|_\infty < 1$, where $\|\cdot\|_\infty$ is the essential supremum. Then there exists a quasiconformal mapping $f : \mathbb{C} \to \mathbb{C}$ whose Beltrami coefficient coincides with μ almost everywhere in $\mathbb{C}$. This mapping is uniquely determined up to a conformal mapping of $\mathbb{C}$ onto itself.*

As a corollary of Lemma F and the Measurable Riemann mapping theorem, we obtain the following corollaries.

Corollary C (see [20, p. 194]). *Let D, D' be bounded simply connected domains in $\mathbb{C}$ and μ a measurable function in D with $\|\mu\|_\infty < 1$. Then there exists a quasiconformal mapping $f : D \to D'$ whose Beltrami coefficient coincides with μ almost everywhere in D. This mapping is uniquely determined up to a conformal mapping of D' onto it self.*

Corollary D (see [2, Lemma 14]). *If μ is a measurable function which satisfies $\|\mu\|_\infty < 1$ and $\overline{\mu(z)} = \mu(1/\overline{z})\overline{z}^2/z^2$. The the restriction of μ-conformal mapping $f^\mu : \mathbb{C} \to \mathbb{C}$ which fixes 0 and 1 to the unit disk, is a $\mu|_{\mathbb{D}}$-conformal self-mapping.*

These corollaries mean that for a given measurable function μ, there exits a unique self μ-conformal mapping of the unit disk which fixes 0 and 1. The Beltrami coefficient of a μ-conformal mapping is invariant under the composition of the conformal mapping. Hence if we have self μ-conformal mappings of the unit disk, then we can obtain μ-conformal mapping from the unit disk to arbitrary simply connected domains by the classical Riemann mapping theorem. Further there are many efficient methods for the numerical conformal mappings (see for example, Porter[31]). Furthermore Ahlfors-Bers[2] investigated f in its dependence on μ. Ahlfors and Bers proved that if μ depends analytically, differentially, or continuously on real parameters, the same is true for f.

2.1.3 Composition and distortion lemmas for quasiconformal mappings

Let μ be a measurable function on a domain D with $\|\mu\|_\infty < 1$ where $\|\cdot\|_\infty$ is essential supremum.

Definition E. *We say a quasiconformal mapping of D is μ-conformal if its Beltrami coefficients coincide with μ almost everywhere in D.*

A μ-comformal mapping is a K_μ-quasiconformal mapping where $K_\mu := (\|\mu\|_\infty + 1)/(\|\mu\|_\infty - 1)$. K_μ is said to be the complex dilatation.

Lemma F ([1, p. 9])**.** *Let μ_i be a measurable function on the domain D_i with $\|\mu_i\|_\infty < 1$ $(i = 1, 2)$. Assume that $f : D_1 \to D_2$ is a μ_f-conformal mapping and $g : D_2 \to D_3$ the μ_g-conformal mapping. Then the following holds:*

1. *$g \circ f$ is a $K_{\mu_f} \times K_{\mu_g}$-quasiconformal mapping.*
2. *If g is conformal, $g \circ f$ is K_{μ_f}-quasiconformal and also μ_f-conformal.*
3. *If g and f are diffeomorphisms, then the chain rule for the Beltrami coefficient*
$$\mu_g \circ f = \frac{f_z}{f_{\overline{z}}} \frac{\mu_{g\circ f} - \mu_f}{1 - \overline{\mu_f} \cdot \mu_{f\circ g}}$$
holds.

In the following we consider the self quasiconformal mappings of the unit disk which fix 0. Mori showed the following distortion theorem for this family.

Lemma G (Mori's Theorem [20, p. 66])**.** *Let $K > 1$ and f be a self K-quasiconformal mapping of the unit disk with $f(0) = 0$. Then for all $z_1, z_2 \in \mathbb{D}$,*
$$|f(z_1) - f(z_2)| \leq 16|z_1 - z_2|^{1/K}$$
holds. The number 16 can't be replaced by any smaller constant which is independent of K.

It was conjectured that the number 16 may be replaced by $16^{1-1/K}$ if we allow dependence on K (see [20, p. 68]).

2.1.4 Normal families of the quasiconformal mappings

We introduce a criterion of the normality for the family of quasiconformal mappings. Let $\mathcal{F}$ be a family of K-quasiconformal mappings of a domain $D \subset \mathbb{C}$.

Lemma H ([20, p. 73]). *The family $\mathcal{F}$ is normal if there exists a positive real number d such that one of the following conditions is satisfied:*

1. *Any quasiconformal mapping $f \in \mathcal{F}$ omits two values whose spherical distance is greater than d.*

2. *Any quasiconformal mapping $f \in \mathcal{F}$ omits one value a and at two fixed points $z_1, z_2 \in D$ takes values such that the distances $k(f(z_1), a), k(f(z_2), a)$ are greater than d.*

3. *Any quasiconformal mapping $f \in \mathcal{F}$ takes values at three fixed points $z_1, z_2, z_3 \in D$ such that the distances $k(f(z_j), f(z_k))\,(j, k = 1, 2, 3, j \neq k)$ are greater than d.*

The limit function f of a sequence of the quasiconformal mappings f_n in the family $\mathcal{F}$ is classified as follows.

Lemma I ([20, p. 74]). *The limit function f of a sequence of K-quasiconformal mappings $f_n \in \mathcal{F}$ convergent in D is either a constant, a mapping of D to two points, or K-quasiconformal mapping of D.*

We will consider the case that the sequence f_n of K-quasiconformal mappings of D converge to a quasiconformal mapping f uniformly on compact subsets of D. If the Beltrami coefficient μ_n of f_n converge to the Beltrami coefficient of f a.e. in D, then we can show that f_n is a good approximation to f in the sense of the definition given by Bers as follows.

Lemma J (Good approximation lemma [20, p. 187]). *Let f_n be a sequence of K-quasiconformal mappings of D which converges to a quasiconformal mapping f with the Beltrami coefficients μ uniformly on compact subsets of D. If the Beltrami coefficients μ_n of f_n tend to a limit μ_∞ almost everywhere in D, then f_n is a good approximation to f, i.e. $\mu_\infty(z) = \mu(z)$ almost everywhere in D.*

2.1.5 Conformal module

We introduce the conformal module of a quadrilateral and its relation to quasiconformal mappings. A quadrilateral consists of a Jordan domain Q

and distinct four boundary points z_1, z_2, z_3, z_4 of Q. We call z_1, z_2, z_3, z_4 the vertices of Q, and shall consider only quadrilaterals $Q(z_1, z_2, z_3, z_4)$ whose sequence of vertices z_1, z_2, z_3, z_4 agrees with the positive orientation with respect to Q. The vertices of a quadrilateral $Q(z_1, z_2, z_3, z_4)$ divide its boundary into four Jordan arcs. We call these the sides of the quadrilateral.

Definition K ([20, p. 21])**.** *Let $Q(z_1, z_2, z_3, z_4)$ be a quadrilateral and set $R_b := \{z \in \mathbb{C} \,|\, 0 < |Re\ z| < 1, 0 < |Im\ z| < b\}$. Then there exists a unique $b > 0$ such that: the conformal map h from $Q(z_1, z_2, z_3, z_4)$ onto $R_b(0, 1, 1 + ib, ib)$ which has the continuous extension to the boundary with $h(z_1) = 0$, $h(z_2) = 1$, $h(z_3) = 1 + ib$, $h(z_4) = ib$ exists. We define the conformal module of $Q(z_1, z_2, z_3, z_4)$ by*

$$M(Q(z_1, z_2, z_3, z_4)) := \frac{1}{b}.$$

We give other representation of the conformal module. Let Γ be a family of curves in the plane such that any curve $\gamma \in \Gamma$ is a countable union of open arcs, closed arcs or closed curves, and every closed subarc is rectifiable. A function ρ defined on the whole plane is called allowable if ρ is a positive valued function, measurable, and satisfies

$$A(\rho) = \int\int_{\mathbb{C}} \rho dx dy \neq 0, \infty.$$

For such a ρ we define

$$L_\gamma(\rho) := \int_\gamma \rho |dz|$$

if ρ measurable on γ, $L_\gamma(\rho) := \infty$ otherwise. Furter let

$$L_\Gamma(\rho) := \inf_{\gamma \in \Gamma} L_\gamma(\rho)$$

for all allowable ρ.

Lemma L ([20, p. 22])**.** *Let $Q(z_1, z_2, z_3, z_4)$ a quadrilateral and $\Gamma_1 \subset \Gamma$ the set of all arcs in $\overline{Q}$ which joins a pair of the arcs $\overset{\frown}{(z_1, z_2)}$ and $\overset{\frown}{(z_3, z_4)}$. Then*

the following equality holds.

$$M(Q(z_1, z_2, z_3, z_4)) = \inf_{\rho} \frac{\int\int_Q \rho dxdy}{L_{\Gamma_1}(\rho)^2}.$$

The conformal module of a quadrilateral was estimated as follows.

Lemma M ([20, p. 23])**.** *Let $Q(z_1, z_2, z_3, z_4)$ be a quadrilateral, $\Gamma_1 \subset \Gamma$ the set of all arcs in $\overline{Q}$ which joins a pair of the arcs $\overset{\frown}{(z_1, z_2)}$ and $\overset{\frown}{(z_3, z_4)}$ and $\Gamma_2 \subset \Gamma$ the set of all arcs in $\overline{Q}$ which joins a pair of the arcs $\overset{\frown}{(z_2, z_3)}$ and $\overset{\frown}{(z_4, z_1)}$. Then the module $M(Q(z_1, z_2, z_3, z_4))$ satisfies the inequality*

$$M(Q) \leq \pi \frac{1 + 2\log(1 + s_1/s_2)}{(\log(1 + 2s_1/s_2))^2}$$

where $s_k = L_{\Gamma_k}(1)$ $(k = 1, 2)$.

2.1.6 Affine linear quasiconformal mappings

Let μ, a, b be complex constants with $a \neq 0$, $|\mu| < 1$. We consider the μ-conformal real-linear mapping

$$L_\mu(z) := \frac{z + \mu\overline{z}}{1 + \mu} \tag{2.1.4}$$

and conformal affine complex-linear mapping

$$H_{a,b}(z) := az + b \tag{2.1.5}$$

for $z \in \mathbb{C}$. Note that L_μ fixes 0 and 1 and hence is determined by its value at any single point. Further $H_{a,b}$ is determined by the images of any two points. For given μ-conformal affine linear mappings, there exists a unique decomposition $H_{a,b} \circ L_\mu$.

Proposition 2.1.1. *Let $z_1, z_2, w_1, w_2 \in \mathbb{C}$ with $z_1 \neq z_2$ and $w_1 \neq w_2$. For a given complex constant $\mu \in \mathbb{D}$, there is a unique μ-conformal affine linear*

mapping $B = B_{\mu;\, z_1,z_2;\, w_1,w_2}$ *which sends* z_i *to* w_i *(*$i = 1, 2$*). This mapping is given by*

$$\begin{aligned} B(z) &= w_1 + \frac{w_2 - w_1}{L_\mu(z_2 - z_1)} L_\mu(z - z_1) \\ &= \frac{L_\mu(z_2 - z)}{L_\mu(z_2 - z_1)} w_1 + \frac{L_\mu(z_1 - z)}{L_\mu(z_1 - z_2)} w_2. \end{aligned}$$

Remark 2.1.2. We note that the coefficients of w_1, w_2 in the last expression are never 0, 1, or ∞ if z_1, z_2, z_3 are distinct.

The following formulation is useful for the later discussion.

Corollary 2.1.3. *Let* $z_i \in \mathbb{C}$ *(*$i = 1, 2, 3$*) noncollinear,* $w_i \in \mathbb{C}$ *(*$i = 1, 2, 3$*) noncollinear and* $\mu \in \mathbb{D}$*. If an* μ*-conformal affine linear map* B *takes* z_1*,* z_2*,* z_3 *to* w_1*,* w_2*,* w_3 *respectively, then the following holds:*

$$\begin{aligned} & w_3 = B(z_3) = \frac{L_\mu(z_2 - z_3)}{L_\mu(z_2 - z_1)} w_1 + \frac{L_\mu(z_1 - z_3)}{L_\mu(z_1 - z_2)} w_2 \\ \iff \quad & L_\mu(z_2 - z_3)\, w_1 + L_\mu(z_3 - z_1)\, w_2 + L_\mu(z_1 - z_2)\, w_3 = 0. \end{aligned} \tag{2.1.6}$$

The Beltrami coefficient of an affine linear mapping can be calculate in the following way.

Corollary 2.1.4. *Let* $z_i \in \mathbb{C}$ *(*$i = 1, 2, 3$*) noncollinear and* $w_i \in \mathbb{C}$ *(*$i = 1, 2, 3$*) noncollinear. There is a unique affine linear mapping which sends* z_i *to* w_i $(i = 1, 2, 3)$*. Further its Beltrami coefficient is equal to*

$$\mu = -\frac{(z_2 - z_1)(w_3 - w_1) - (z_3 - z_1)(w_2 - w_1)}{(\overline{z_2} - \overline{z_1})(w_3 - w_1) - (\overline{z_3} - \overline{z_1})(w_2 - w_1)}. \tag{2.1.7}$$

2.2 Simplicial approximation and least squares

In this section, we will introduce the basic facts about the simplicial approximation. Also we define the least square solution, and show a condition for its uniqueness.

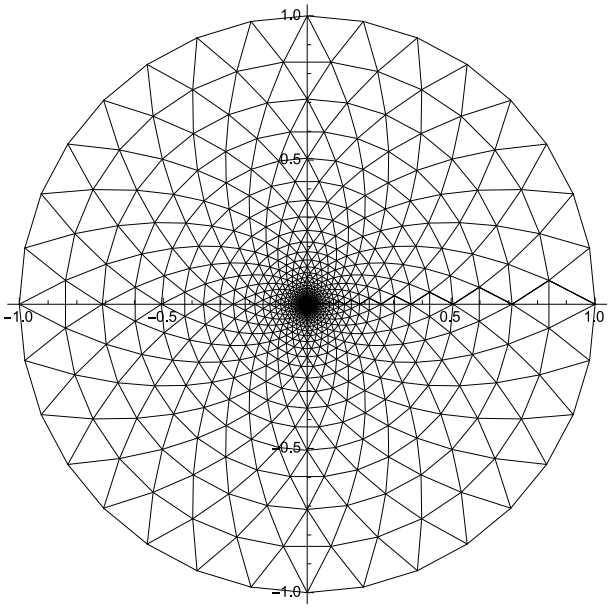

Figure 2.2.1: An triangulation of the unit disk which consists of 16×16.

2.2.1 Triangulation and piecewise linear mapping

We define the triangulation of the unit disk as the following.

Definition N. *We say a Euclidian simplicial complex T which consist of finite closed 2-simplices $\{\tau_i\}$ in $\mathbb{C}$ forms a triangulation of the unit disk $\mathbb{D}$ if:*

1. *$P := |T|$ is a closed simple jordan polygon whose vertices lie on the boundary of the unit disk $\partial\mathbb{D}$, where $|T|$ is the union of all 2-simplices in T.*

2. *each 1-face l_k of any 2-simplex τ_i of T is either:*

   - *an edge of P, or*
   - *there exists unique $j (j \neq i)$ such that l_k is an edge of a 2-simplex τ_j in T.*

A example of the triangulation of the unit disk is drawn in Figure 2.2.1.

We will approximate a quasiconformal mapping by the piecewise linear mapping which is induced by two triangulations of the unit disk.

Definition O. *Let T_z, T_w be triangulations of $\mathbb{D}$. If T_z and T_w are simplicially equivalent, then the piecewise linear mapping $f : |T_z| \to |T_w|$ which sends 2-simplex in T_z to the corresponding 2-simplex in T_w linearly, is a homeomorphism between $|T_z|$ and $|T_w|$. We say f is the induced piecewise mapping by T_z and T_w.*

The Beltrami coefficients of f is defined on each interior of the 2-simplex and the values are determined as in Corollary 2.1.4. We will use the notation $PL(T_z)$ for the space of the piecewise linear mappings for T_z, i.e.

Definition P. *For given triangulation of the unit disk T_z, we define $PL(T_z)$ by*

$$\{f : |T_z| \to \mathbb{C} \,|\, f \text{ is continuous on } |T_z|, \text{ and linear on each 2-simplex in } T_z\}.$$

The following Lemma 2.2.1 is important for proof of our main theorem.

Lemma 2.2.1. *Let $T_z := \{\tau_j\}$ be a triangulation of the unit disk $\mathbb{D}$ such that $P_z := |T_z|$ is a simple polygon with k vertices. Suppose $f : |T_z| \to \mathbb{D} \in PL(T_z)$ preserves the orientation on each $\tau \in T_z$ and maps $\partial|T_z|$ homeomorphically to a boundary of a simple polygon P_w with k vertices on the unit circle. Then the secant map induced by f and T_z, is an orientation preserving homeomorphism from P_z to P_w. It means that the collections of 2-simplicies $T_w := \{f(\tau)\}_{\tau \in T_z}$ is a simplicial complex, and form a triangulation of the unit disk.*

Proof. At first, we will prove $f(\operatorname{Int} P_z) \subseteq \operatorname{Int} P_w$ where $\operatorname{Int} P_z$, $\operatorname{Int} P_w$ are the interior of P_z, P_w, respectively. If the assumption is false, the boundary of $f(\operatorname{Int} P_z)$ would contain a point p exterior to $\operatorname{Int} P_w$, and there would be a sequence $\{z_n\} \subset \operatorname{Int} P_z$ such that $f(z_n) \to p$. Now z_n must accumulate in the closure of $\operatorname{Int} P_z$, and in fact z_n converge to a boundary point $z \in \partial P_z$ since f is a local homeomorphism. Thus z_0 is on an edge of a 2-simplex joining two vertices on $\partial\mathbb{D}$, and p is on the corresponding edge of the image 2-simplex, which by the hypothesis on boundary points must lie in ∂P_z, a contradiction which proves $f(\operatorname{Int} P_z) \subseteq \operatorname{Int} P_w$. A similar argument yields that $\operatorname{Int} P_w \subseteq f(\operatorname{Int} P_z)$, and we have $f(P_z) = P_w$. f satisfies the path-lifting

property, and thus is a covering map of simply connected regions, so it is a orientation preserving homeomorphism. □

2.2.2 Secant mapping and least squares

Next we define the secant map for the C^1 diffeomorphism and triangulation of the unit disk. The secant map is also used in the proof of our main theorem.

Definition Q (see [29, p. 90]). *Let T_z be a triangulation of $\mathbb{D}$ and $f : \mathbb{D} \to \mathbb{C}$ a C^r map where $r \in \mathbb{N}$. For any 2-simplex $\tau \in T_z$, the linear map $L_{f,\tau} : \tau \to \mathbb{C}$ which is equal to $f(v_{j,k})$ on the all vertices of $v_{j,k}$ of τ, is called the secant map which is induced by f and τ. Similarly we say that, the piecewise linear mapping $L_{f,T_z} : |T_z| \to \mathbb{C}$ is the secant map which is induced by f and T_z, if the all restrictions of L_{f,T_z} to 2-simplex $\tau \in T_z$ is the secant map which is induced by f and τ.*

The secant map induced by f and T_z is an element of $PL(T_z)$. We will use the least squares method in our algorithm which will be presented later. $\boldsymbol{M}_{m,n}(\mathbb{C})$ shall denote the complex $m \times n$ matrix.

Definition R ([5, p. 2]). *Let $m, n \in \mathbb{N}$ with $m > n$. Let $\boldsymbol{AW} = \boldsymbol{B}$ be an overdetermined linear system with $\boldsymbol{A} \in \boldsymbol{M}_{m,n}(\mathbb{C})$, $\boldsymbol{B} \in \mathbb{C}^m$ and unknown vector $\boldsymbol{W} \in \mathbb{C}^n$. We will write this linear system as $(\boldsymbol{A}, \boldsymbol{B})$. This linear system usually has no solution, and we consider the quadratic minimization problem: Find a $\boldsymbol{W} \in \mathbb{C}^n$ which minimizes $\|\boldsymbol{AW} - \boldsymbol{B}\|_2$. If such $\boldsymbol{W}$ exists, we call it the least squares solution of the linear system $(\boldsymbol{A}, \boldsymbol{B})$.*

The following condition for the existence and uniqueness for the least square solution is well known.

Lemma S ([5, Theorem 1.2.10]). *In the same setting as Definition R, if $\boldsymbol{A}$ has full column rank, then there exists a least square solution of the linear system $(\boldsymbol{A}, \boldsymbol{B})$ and it is unique.*

There are many efficient numerical methods for the least squares problem. See [5] for the details.

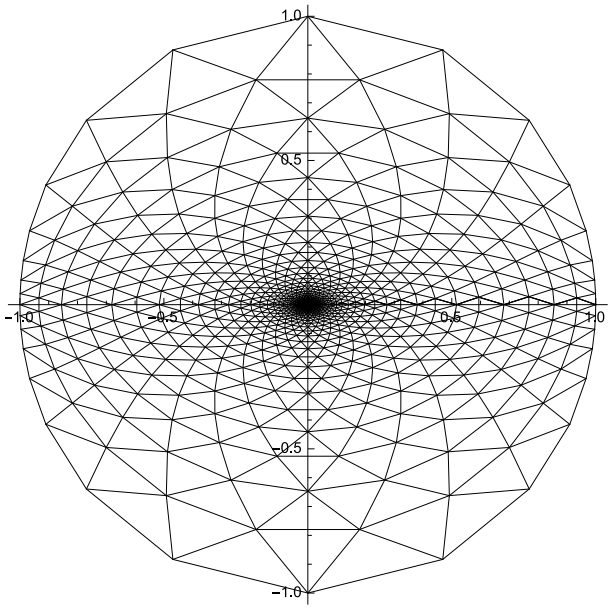

Figure 2.2.2: A triangulation of the unit disk which is simplicially equivalent to Figure 2.2.1

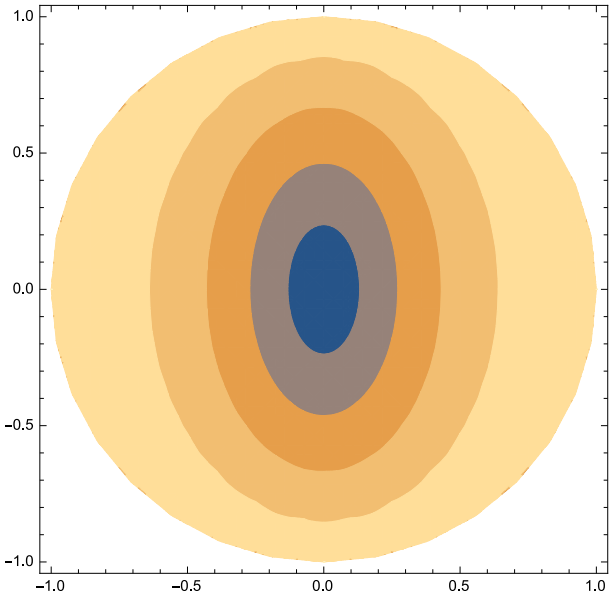

Figure 2.2.3: The contour plot of the absolute values for the induced PL mapping by Figure 2.2.1 and Figure 2.2.2

Chapter 3

Algorithm for quasiconformal mappings

In this chapter, we will propose a numerical method for the quasiconformal mappings. As we mentioned in Chapter 2, we will concentrate on the numerical construction for the normalized self μ-conformal mapping of the unit disk.

3.1 Setting

Corollary D stated that: For given measurable function μ on $\mathbb{D}$ with $\|\mu\|_\infty < 1$, there exists a unique self μ-conformal mapping f^μ of the unit disk which fixes 0 and 1. We will propose an algorithm to produce triangulations of the unit disk T_z, T_w whose vertices include 0 and 1, so that the induced piecewise linear mapping $f_{\mu,T_z} \in PL(T_z)$ approximate f in the following sense: the Beltrami coefficient μ' of the induced piecewise linear mapping $f_{\mu,T_z} \in PL(T_z)$ reduces $\|\mu - \mu'\|_\infty$ on each $\tau \in T_z$.

3.2 Discrete Beltrami equation

Let μ be a measurable function with $\|\mu\|_\infty < 1$. First we propose a discrete version of the Beltrami equation (2.1.3).

3.2.1 Logarithmic coordinates

We take logarithmic coordinates in the form of the variables $Z = \log z$, $W = \log w$ in the left half-plane (cf. [20, section 6.4]), and extend the mapping to the right half-plane symmetrically by the chain rule of the Beltrami coefficient which is mentioned in Chapter 2. First we will approximate

$$W = F(Z) \tag{3.2.1}$$

where $F(Z) = \exp \circ f(\log Z)$, and then apply the operation

$$z = \exp(Z), \quad w = \exp(W) \tag{3.2.2}$$

to obtain the desired mapping $z \mapsto w$. Afterwards we will justify the distortion of triangles produced by the exponential mapping does not affect the accuracy significantly.

3.2.2 Domain of definition and triangulation

Take $M, N \in \mathbb{N}$ and let $R_{-m} \in \mathbb{R}$ ($m \in \{0, 1, 2, \cdots, M\}$) so that

$$R_{-M} < R_{-M+1} < \cdots < R_{-1} < R_0 = 0.$$

Further we define $(M+1)N$ vertices

$$Z_{j,k} = R_j + \frac{2\pi(k + (j \bmod 2)/2)}{N} i \tag{3.2.3}$$

for $-M \leq j \leq 0$ and $0 \leq k \leq N-1$. (If we want to extend the formula for arbitrary values of k, we have a periodic mesh with $Z_{j,k+N} = Z_{j,k} + 2\pi N i$). Our mesh contains $M \times N$ *rightward pointing* 2*-simplices* defined by

$$\tau^+_{j,k} = \begin{cases} \mathrm{Conv}(Z_{j-1,k-1},\ Z_{j-1,k},\ Z_{j,k}), & j \text{ even}, \\ \mathrm{Conv}(Z_{j-1,k},\ Z_{j-1,k+1},\ Z_{j,k}), & j \text{ odd}, \end{cases} \tag{3.2.4}$$

for $-M+1 \le j \le 0$ where $\mathrm{Conv}(Z_1, Z_2, Z_3)$ is the 2-simplex which vertices are Z_1, Z_2, Z_3. There are also $M \times N$ *leftward pointing* 2*-simplices*

$$\tau^-_{j,k} = \begin{cases} \mathrm{Conv}(Z_{j+1,k-1},\ Z_{j+1,k},\ Z_{j,k}), & j \text{ even}, \\ \mathrm{Conv}(Z_{j+1,k},\ Z_{j+1,k+1},\ Z_{j,k}), & j \text{ odd}, \end{cases} \tag{3.2.5}$$

for $-M \le j \le -1$. For even values of j the 2-simplex $\tau^+_{j,0}$ contains $Z_{j-1,-1}$ and the 2-simplex $\tau^-_{j,0}$ contains $Z_{j+1,-1}$; while for odd j the 2-simplex $\tau^+_{j,N-1}$ contains $Z_{j-1,N}$ and the 2-simplex $\tau^-_{j,N-1}$ contains $Z_{j+1,N}$. The second index k of each of these points lies outside of the basic range $0 \le k \le N-1$. We treat

$$T_{M,N} := \{\tau^\pm_{j,k}\}$$

as a simplicial complex and solve the Beltrami equation on $T_{M,N}$.

To simplify the following discussion, we set

$$R_j := \frac{\sqrt{3}\,\pi\, j}{N}. \tag{3.2.6}$$

In this case, the triangles $\tau^\pm_{jk}$ are equilateral. We extend this mesh symmetrically to the right half-plane as

$$Z_{j,k} = \varrho(Z_{-j,k})$$

where ϱ is the reflection at the imaginary axis

$$\varrho(Z) = -\overline{Z}. \tag{3.2.7}$$

Now we have $(2M+1)N$ vertices and $4MN$ 2-simplices. We say this is the basic mesh in the logarithmic coordinates.

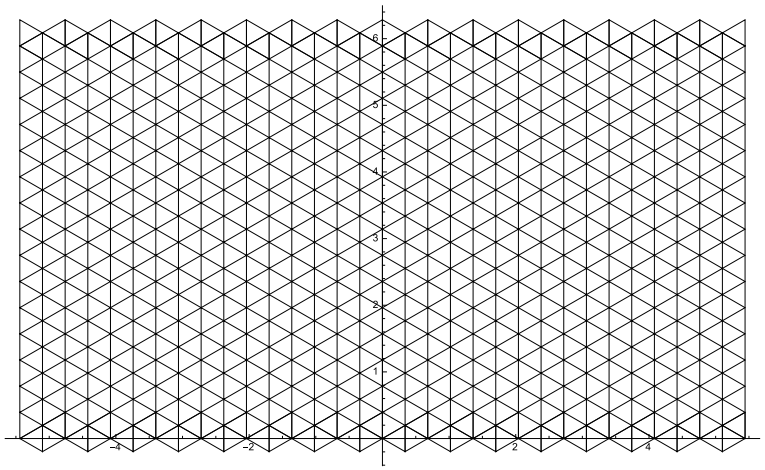

Figure 3.2.1: The basic mesh in the logarithmic coordinates with 16×16 equilateral triangles

3.2.3 Beltrami coefficients in the logarithmic coordinates

We consider the Beltrami coefficients of $F(Z)$. By Lemma 2.1.4, the Beltrami coefficients of $F(Z)$ are given as follows:

$$\nu(Z) = \mu(e^Z)\frac{e^{\overline{Z}}}{e^Z} = \mu(e^Z)e^{-2i\,\mathrm{Im}\,Z}, \quad \mathrm{Re}\,Z < 0. \tag{3.2.8}$$

Using ν, we set the Beltrami coefficients as $\nu(Z) = \overline{\nu(\varrho(Z))}$ for $\mathrm{Re}\,Z > 0$. Corresponding $F(Z) = \rho(F(\rho(Z))$ have the symmetry with respect to the imaginary axis. We will write $\nu_{j,k}^{\pm}$ for the average value of $\nu(Z)$ on the 2-simplices $\tau_{j,k}^{\pm}$. It is useful for the upcoming numerical work to take the average of $\nu(Z)$ over the three vertices as an approximation of this average, at least when ν is continuous. Let us note that

$$\nu_{jk} = \overline{\nu_{-j,k}}, \quad j > 0. \tag{3.2.9}$$

3.2.4 Triangle equations

For all rightward pointing 2-simplicies $\tau^+_{jk} \in T_{M,N} := \{\tau^{\pm}_{j,k}\}$ in the left half plane, we construct the following MN linear equations by Corollary 2.1.3:

$$a^+_{jk}W_{jk} + b^+_{jk}W_{j-1,k} + c^+_{jk}W_{j-1,k+1} = 0 \tag{3.2.10}$$

where

$$\begin{aligned}
a^+_{jk} &= \begin{cases} L_{\nu_{jk}}(Z_{j-1,k-1} - Z_{j-1,k}), & j \text{ even}, \\ L_{\nu_{jk}}(Z_{j-1,k} - Z_{j-1,k+1}), & j \text{ odd}, \end{cases} \\
b^+_{jk} &= \begin{cases} L_{\nu_{jk}}(Z_{j-1,k} - Z_{j,k}), & j \text{ even}, \\ L_{\nu_{jk}}(Z_{j-1,k+1} - Z_{jk}), & j \text{ odd}, \end{cases} \\
c^+_{jk} &= \begin{cases} L_{\nu_{jk}}(Z_{j,k} - Z_{j-1,k-1}), & j \text{ even}, \\ L_{\nu_{jk}}(Z_{jk} - Z_{j-1,k}), & j \text{ odd}. \end{cases}
\end{aligned} \tag{3.2.11}$$

Further MN linear equations for the leftward pointing 2-simplices τ^-_{jk} in the left half plane are constructed Corollary 2.1.3,

$$a^-_{jk}W_{jk} + b^-_{jk}W_{j+1,k-1} + c^-_{jk}W_{j+1,k} = 0 \tag{3.2.12}$$

where

$$\begin{aligned}
a^-_{jk} &= \begin{cases} L_{\nu_{jk}}(Z_{j+1,k-1} - Z_{j+1,k}), & j \text{ even}, \\ L_{\nu_{jk}}(Z_{j+1,k} - Z_{j+1,k+1}), & j \text{ odd}, \end{cases} \\
b^-_{jk} &= \begin{cases} L_{\nu_{jk}}(Z_{j+1,k} - Z_{j,k}), & j \text{ even}, \\ L_{\nu_{jk}}(Z_{j+1,k+1} - Z_{j,k}), & j \text{ odd}, \end{cases} \\
c^-_{jk} &= \begin{cases} L_{\nu_{jk}}(Z_{j,k} - Z_{j+1,k-1}). & j \text{ even}, \\ L_{\nu_{jk}}(Z_{j,k} - Z_{j+1,k}), & j \text{ odd}. \end{cases}
\end{aligned} \tag{3.2.13}$$

We note that these equations stand as written for all 2-simplices in the left half plane. Further we must take the $2\pi i$-periodicity into account in order to conserve our requirement that $0 \leq l \leq N-1$ in every appearance of $W_{j,l}$.

If $k+1 = N+1$ in (3.2.10) and $k-1 = -1$ in (3.2.12), the exceptions

to these equations occur. We have to use $W_{j\pm1,N-1} - 2\pi i$ instead of $W_{j\pm1,-1}$ when $k = 0$ and j is even. Also when $k = N-1$ and j is odd, we write $W_{j\pm1,0} + 2\pi i$ instead of $W_{j\pm1,N}$. Considering (3.2.4) and (3.2.5), we define the exceptional equations as:

$$\begin{aligned} a^{\pm}_{j0}W_{j0} + b^{\pm}_{j0}W_{j-1,0} + c^{\pm}_{j0}W_{j-1,1} &= -2\pi i c^{\pm}_{j0}, \quad j \text{ even}, \\ a^{\pm}_{j0}W_{j0} + b^{\pm}_{j0}W_{j-1,0} + c^{\pm}_{j0}W_{j-1,1} &= 2\pi i b^{\pm}_{j0}, \quad j \text{ odd}. \end{aligned} \tag{3.2.14}$$

Now we consider these equations in the right half-plane via (3.2.7). We want F to be symmetric with respect to the imaginary axis, i.e. $F = \varrho F \varrho$. The Beltrami coefficients of $\varrho F \varrho$ is $\nu = \overline{\nu} \circ \varrho$, and hence we reflect ν appropriately to the right half-plane as discrete Beltrami coefficients like (3.2.9). It means that, for a 2-simplex $\tau^{\pm}_{jk} = \varrho(\tau^{\pm}_{-j,k})$ in the right half Z-plane ($j \geq 0$), the image $F(\tau^{\pm}_{j,k})$ in the W-plane, defined by $W_{j,k}$ and two adjacent vertices should be the same as $\varrho(F(\tau^{\pm}_{-j,k}))$. Hence the correspondence $\varrho(\tau^{\pm}_{jk}) \to \varrho(F(\tau^{\pm}_{jk}))$ translates into equations of the same form as (3.2.10), (3.2.12) with $j \geq 0$ and with the coefficients

$$a^{\pm}_{jk} = \overline{a^{\pm}_{-j,k}}, \; b^{\pm}_{jk} = \overline{b^{\pm}_{-j,k}}, \; c^{\pm}_{jk} = \overline{c^{\pm}_{-j,k}}. \tag{3.2.15}$$

We have totally $4MN$ triangle equations for the simplices of $T_{M,N}$.

3.2.5 Boundary equations

The image of left boundary vertices $\{Z_{M,k}\}$, are lie on a circle $\mathcal{C}$ which is centered at the origin and has the radius $r_{-M} = \exp(R_{-M})$. Originally, the image of the infinitesimal circle by a quasiconformal mapping is the infinitesimal ellipse. The shape of this ellipse depends on the Beltrami coefficients at the origin. If the quasiconformal mapping f is C^1 at the origin and r_{-M} is small enough, the image $f(\mathcal{C})$ approximately forms an ellipse (considering the Taylor expansion of f, the image is close to the ellipse by linear term). Under this situation, we will add the following equations.

Let e_k be the images of these points $\{Z_{m,k}\}$ under the real-linear mapping

$L_{\mu(0)}$, i.e.

$$e_k = L_{\mu_0}(r_{-M}e^{2\pi ik/N}) = r_{-M}L_{\mu_0}(e^{2\pi ik/N}), \quad 0 \le k \le N-1,$$

where μ_0 denotes the average value of $\mu(z)$ inside this circle. These vertices lie on an ellipse, however it dose not correspond to the image by the quasi-conformal mapping in general, but the shape is the same infinitesimally. In other words, we want a condition that the image of $\mathcal{C}$ is an unknown complex nonzero constant multiple of the ellipse $\{e_k\}$. Here we consider the image of the vertices in the logarithmic coordinates:

$$E_k = \log e_k \tag{3.2.16}$$

with $0 \le \arg E_k < 2\pi$. The condition above states that the image of the curve $\{Z_{-M,k}\}_k$ is a translate of the curve $\{E_k\}_k$ by a complex constant. The same argument holds for the reflected curve $\{\varrho(E_k)\}_k$. Hence the boundary equations which achieve the above condition are the following $2(N-1)$ equations

$$\begin{aligned} W_{-M,k} - W_{-M,k-1} &= D_k, \\ W_{M,k} - W_{M,k-1} &= \overline{D_k}, \end{aligned} \tag{3.2.17}$$

where $D_k = E_k - E_{k-1}$ and $1 \le k \le N-1$. The magnitude of r_{-M} does not influence the value of D_k.

3.2.6 Normalization

Finally, we add an equation. We want a normalized μ-conformal mapping which fixes 0 and 1. For normalization that $f(1) = 1$, we set

$$W_{0,0} = 0. \tag{3.2.18}$$

3.3 Associated linear system

In the argument above, we construct totally $n_{\mathrm{e}} = 4MN + 2(N-1) + 1$ complex linear equations for the $n_{\mathrm{v}} = (2M+1)N$ unknown variables W_{jk}, $-M \leq j \leq M$, $0 \leq k \leq N-1$. Let $p = p(j,k)$ be an fixed bijection from the set of index pairs $\{(j,k)\}$ to the range $1 \leq p \leq n_{\mathrm{v}}$. Using this bijection p, we will rename the variables in a single vector $\boldsymbol{W}$ with

$$\boldsymbol{W} := W_p = W_{jk} \tag{3.3.1}$$

for convenience. The linear system now takes the form:

$$\boldsymbol{AW} = \boldsymbol{B} \tag{3.3.2}$$

where $\boldsymbol{A} = (A_{j,k})$ is the $n_{\mathrm{e}} \times n_{\mathrm{v}}$-type complex matrix and $\boldsymbol{B} = (B_k)$ is a complex vector of length n_{e}. When we take a pair of N, M, the mesh $\{Z_{jk}\}$ is fixed, and linear system above is defined. We will say that this linear system $(\boldsymbol{A}, \boldsymbol{B})$ is the *associated linear system* to the collection of ν-values $\{\nu_{jk}\}$. The coefficients depend both on ν_{jk} and Z_{jk}.

3.4 Approximation of the solution

Since our linear system is overdetermined, we chose the standard least squares method for the approximation.

3.4.1 Least squares solution

Given arbitrary $T_{M,N}$ and the measurable Beltrami coefficients μ, the following Lemma holds for the corresponding associated linear systems $(\boldsymbol{A}, \boldsymbol{B})$.

Lemma 3.4.1. *Let $\boldsymbol{X}$ be a complex vector which length is the same as the number of unknown variables n_{v}. If $\boldsymbol{AX} = 0$, then $\boldsymbol{X} = 0$.*

Proof. Take $\boldsymbol{X} \in \mathbb{C}^{n_{\mathrm{v}}}$ and assume that $\boldsymbol{AX} = 0$. We write $X_{j,k}$ for $X_{p(j,k)}$ as mentioned before. First consider equations (3.2.17) for the boundary

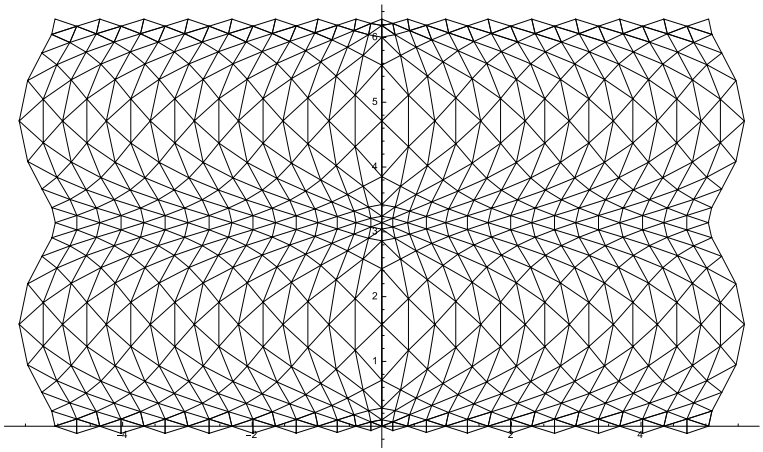

Figure 3.4.1: The corresponding simplicial complex for the Beltrami coefficients $\mu(z) = 0.3$ and the basic mesh in the logarithmic coordinates in Figure 3.4.1

condition, with zero on the right hand side in place of D_k and $\overline{D_k}$. These equations are of the form $X_{-M,k+1} - X_{-M,k} = 0$, and hence all $X_{-M,k}$ are the same value. Next we consider the triangle equations for the rightward-pointing 2-simplices (3.2.10), (3.2.14) with $j = -M + 1$:

$$a^+_{-M+1,k} X_{-M+1,k} + b^+_{-M+1,k} X_{-M,k} + c^+_{-M+1,k} X_{-M,k'} = 0$$

for suitable k'. Considering $a^+_{-M+1,k} \neq 0$ (recalling the remark after Proposition 2.1.1) and $a^+_{-M+1,k} + b^+_{-M+1,k} + c^+_{-M+1,k} = 0$, we obtain $X_{-M+1,k} = c$ for all k. Similarly we have $X_{-j,k} = c$ for all k and $-M \leq j \leq 0$. Further the normalization condition $X_{0,0} = 0$ means that $c = 0$. Therefore the symmetry gives $X_{j,k} = 0$ for all j, k. In conclusion, we obtain $\boldsymbol{X} = 0$. □

The Lemma states that the matrix $\boldsymbol{A}$ has full column rank. Therefore we have the following uniqueness for our least squares solution.

Lemma 3.4.2. *The least squares solution $\boldsymbol{W} = \{W_{j,k}\}$ ($-M \leq j \leq M$, $0 \leq k \leq N-1$) of the associated linear system $(\boldsymbol{A}, \boldsymbol{B})$ exists uniquely. Furthermore $\boldsymbol{W}$ satisfies the following symmetric relation:*

$$\boldsymbol{A}\overset{\leftrightarrow}{\boldsymbol{W}} = \boldsymbol{A}\varrho(\boldsymbol{W})$$

where $\overset{\leftrightarrow}{W}_{jk} = W_{-j,k}$, $\varrho(\boldsymbol{W}) = \{\varrho(W_{jk})\}$ *and* ρ *is defined by* (3.2.7), *i.e. the entries of* $\boldsymbol{W}$ *satisfy the symmetry* $W_{-j,k} = \rho(W_{jk})$. *In particular, the values* $\{W_{0,k}\}$ *are purely imaginary.*

Proof. By Lemma 3.4.1 and Lemma S, $\boldsymbol{A}$ has full column rank, so this optimal $\boldsymbol{W}$ is unique. For any $\boldsymbol{W} \in \mathbb{C}^{n_{\mathrm{v}}}$, the relation $\boldsymbol{A}\underline{\overset{\leftrightarrow}{\boldsymbol{W}}} = \boldsymbol{A}\underline{\varrho(\boldsymbol{W})}$ follows immediately from the above symmetric construction as (3.2.15). Therefore $\overset{\leftrightarrow}{\boldsymbol{W}} = \varrho(\boldsymbol{W})$. □

3.4.2 Exponential mapping

Finally, we apply the exponential mapping to the vertices of $\{Z_{j,k}\}$ and $\{W_{j,k}\}$, and then we take the piecewise linear mapping which is induced by the corresponding between the two simplices.

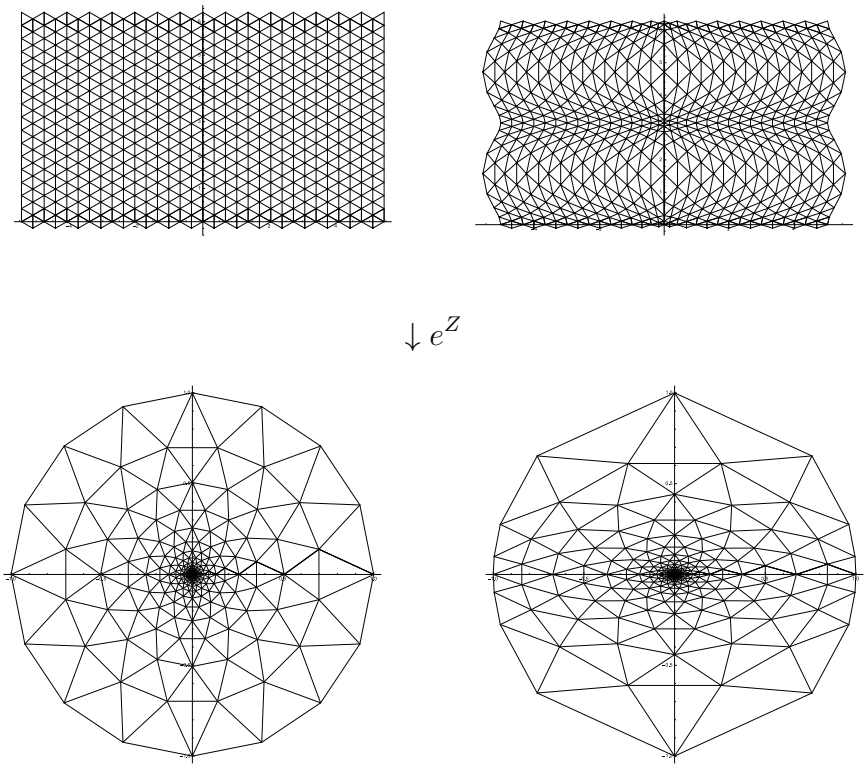

Figure 3.4.2: The piecewise linear approximation for the quasiconformal mapping whose Beltrami coefficients are $\mu(z) = 0.3$ with $M = N = 16$

Chapter 4

Convergence

In this chapter we will give a justification of our algorithm. The algorithm is summarized as follows.

Algorithm 1 Piecewise linear approximation of a quasiconformal mapping

Input: The measurable function $\mu : \mathbb{D} \to \mathbb{C}$ with $\|\mu\|_\infty < 1$ and dimensions M, N for a simplicial complex $T_{M,N}$ in the logarithmic coordinates.
1. Calculate the averages of the Beltrami coefficients $\nu_{j,k}$ on each triangle in the logarithmic coordinates via (3.2.8). (If μ is continuous on the unit circle, we may use averages on the 3 vertices.)
2. Calculate the coefficients of the associated linear system $(\boldsymbol{A}, \boldsymbol{B})$ of $\{\nu_{jk}\}$ and $T_{M,N}$ as prescribed by equations (3.2.10), (3.2.12), (3.2.14), (3.2.17), and (3.2.18).
3. Calculate the least squares solution $\boldsymbol{W}$ to the associated linear system $(\boldsymbol{A}, \boldsymbol{B})$, and arrange the entries of $\boldsymbol{W}$ to form the mesh $\{W_{jk}\}$. (The least squares solution exists uniquely by Lemma 3.4.2.)
4. Calculate $w_{jk} = \exp W_{jk}$ for $-M \le j \le 0$ and $0 \le k \le N-1$.
Output: The piecewise linear mapping such that $z_{jk} \mapsto w_{jk}$ where $z_{jk} = \exp Z_{jk}$.

We will discuss the convergence properties of this approximations for $\mu \in C^1(\mathbb{D})$.

4.1 Convergence of the approximations

Here we state our main theorem for our algorithm.

Theorem 4.1.1. *Let $s \in \mathbb{N}$ and $M_s, N_s \in \mathbb{N}$ be strictly increasing sequences which satisfy*

$$c_1 N_s \log N_s \leq M_s \leq c_2 N_s \log N_s \tag{4.1.1}$$

for constants c_1, c_2 where $c_1 > 1/(\pi\sqrt{3})$. If the given Beltrami coefficient is in the class C^1 with $\|\mu\|_\infty = c_3 < 1$, then the following holds.

i. If s is large enough, the points $\{z_{j,k}^{(s)}\}$ and the points $\{w_{j,k}^{(s)}\}$ produced by the algorithm form the vertex sets of triangulations $T_z^{(s)}$ and $T_w^{(s)}$ of the unit disk $\mathbb{D}$. Furthermore, for any fixed compact set $K \subset Int\ \mathbb{D}$, $K \subset |T_z^{(s)}|$ and $K \subset |T_w^{(s)}|$ hold when s is large enough.

ii. The mappings f_s converge to the μ-conformal mapping f normalized by $f(0) = f(1) - 1 = 0$ uniformly on compact subsets of $\mathbb{D}$ as $s \to \infty$.

Remark 4.1.2. We conjecture that the condition $\mu \in C^1$ is overly restrictive by the numerical experiments in the next chapter.

Proof. Let μ be a C^1-function and take strictly increasing sequences $\{M_s\}$, $\{N_s\} \subset \mathbb{N}$ with the growth condition $c_1 N_s \log N_s \leq M_s \leq c_2 N_s \log N_s$ for constants c_1, c_2 where $c_1 > 1/(\pi\sqrt{3})$. For a fixed s, let $(\boldsymbol{A}_s, \boldsymbol{B}_s)$ be the associated linear system, $\{Z_{j,k}^{(s)}\}$ be the vertices of the basic mesh $T_Z^{(s)}$ in the logarithmic coordinates and $\{W_{j,k}^{(s)}\}$ the least squares solutions of $(\boldsymbol{A}_s, \boldsymbol{B}_s)$. Further let $\nu_s := \{(\nu_{j,k}^{\pm})^{(s)}\}$ denote the collection of average values of the function ν which are defined by (3.2.8) on the triangles of $T_Z^{(s)}$. We will divide the proof into several steps.

Step 1. We will replace $\mu(z)$ with $\mu(rz)$ for $r < 1$ arbitrarily close to 1, and then apply the standard approximation arguments. Thus we assume that $\mu(z)$ belongs to the class C^1 on a neighborhood of the closed unit disk. This condition implies that the corresponding normalized μ-conformal mapping f is in the class C^2. The Beltrami coefficient in the logarithmic coordinate ν belongs to the class C^1 in a neighborhood of the closed left half-plane and has period $2\pi i$, while the corresponding $F(Z) = \log f(\exp Z)$ is in C^2 there. Note that in general the extension of F by reflection in the imaginary axis is not in C^1 on the imaginary axis.

Step 2. Let $\{z_{j,k}^{(s)}\} := \{\exp Z_{j,k}^{(s)}\}$. Considering the growth condition (4.1.1), we have

$$r_{-M_s} := e^{\mathrm{Re}\ Z_{-M_s,k}} = e^{-(\pi\sqrt{3}c_1)\log N_s} = N_s^{-\pi\sqrt{3}c_1} \tag{4.1.2}$$

since $\pi\sqrt{3}c_1 > 1$. Furthermore we see that

$$|z_{-M_s,k} - z_{-M_s,k-1}| = 2r_{-M_s}\sin\frac{\pi}{N_s} < \frac{2\pi r_{-M_s}}{N_s} = O(1/N_s^{1+\pi\sqrt{3}c_1}).$$

Step 3. Let $\{Z_{j,k}^{(s)}\}, \{W_{j,k}^{(s)}\}$ be the vertices of the simplicial complex $T_Z^{(s)}, T_W^{(s)}$ in the logarithmic coordinates which are produced by our algorithm. If the equations

$$\boldsymbol{A}_s\boldsymbol{W}_s = \boldsymbol{B}_s$$

hold, the piecewise linear mapping $F_s : |T_Z^{(s)}| \to |T_W^{(s)}|$ is exactly ν_s-conformal. However it does not hold in general. Hence we take the least squares solution for the associated linear system $(\boldsymbol{A}_s, \boldsymbol{B}_s)$. $\boldsymbol{W}_s$ minimizes the L_2-norm $\|\boldsymbol{R}_s\|_2$ of the residual vector

$$\boldsymbol{R}_s = \boldsymbol{A}_s\boldsymbol{W}_s - \boldsymbol{B}_s. \tag{4.1.3}$$

Now we consider another linear system. Let $\boldsymbol{W}_s^*$ be defined by

$$\boldsymbol{W}_s^* := \{W_{j,k}^{*(s)}\} = \{F(Z_{j,k}^{(s)})\} \tag{4.1.4}$$

which contains the images of the vertices under the true ν-conformal mapping $F(Z) = \log f(e^Z)$. Let F_s^* be the secant map which is induced by $\{Z_{j,k}^{(s)}\}$ and F, and let ν_s^* be the Beltrami coefficient of F_s^*. The associated linear system $(\boldsymbol{A}_s, \boldsymbol{B}_s)$ used in the algorithm is defined in terms of the values of ν_s. By the construction, F_s^* coincides with F on the vertices of $\{Z_{j,k}^{(s)}\}$. However the Beltrami coefficient of F_s^* is constant on each 2-simplex. Let $(\boldsymbol{A}_s^*, \boldsymbol{B}_s^*)$ be the associated linear system which is induced by $T_Z^{(s)}$ and ν_s^*. We will consider the following linear systems:

$$\boldsymbol{A}_s\boldsymbol{W}_s - \boldsymbol{B}_s = \boldsymbol{R}_s, \tag{4.1.5}$$

$$\boldsymbol{A}_s^*\boldsymbol{W}_s^* - \boldsymbol{B}_s^* = \boldsymbol{\varepsilon}_s. \tag{4.1.6}$$

The complex vector $\boldsymbol{\varepsilon}_s$ in (4.1.6) is defined in the next step.

Step 4. The entries of $\boldsymbol{\varepsilon}_s$ corresponding to the the triangle equations are 0 because F_s^* is ν_s^*-conformal. This means that the nonzero elements of $\boldsymbol{\varepsilon}_s$ are in the position of boundary equations. Considering (3.2.17), the values in $\boldsymbol{A}_s^*\boldsymbol{W}_s^*$ are $F(Z_{-M,k}^{(s)}) - F(Z_{-M,k-1}^{(s)})$ and the values in $\boldsymbol{B}_s^*$ are $E_k^{(s)} - E_{k-1}^{(s)}$. Hence the corresponding positions in $\boldsymbol{\varepsilon}_s$ contain the values

$$(F(Z_{-M,k}^{(s)}) - E_k^{(s)}) - (F(Z_{-M,k-1}^{(s)}) - E_{k-1}^{(s)}).$$

We will estimate this by the regularity of f. Since f is in the class C^2 and the approximation

$$\begin{aligned} f(z) &= f_z(0)z + f_{\overline{z}}(0)\overline{z} + O(|z|^2) \\ &= aL_{\mu(0)}(z) + O(|z|^2) \end{aligned}$$

holds near the origin, where a is some non-zero constant. Therefore

$$\begin{aligned} \frac{f(z_{-M_s,k}^{(s)})e_{k-1}^{(s)}}{f(z_{-M_s,k-1}^{(s)})e_k^{(s)}} &= \frac{(ae_k^{(s)} + O(r_{-M_s}^2))(e_{k-1}^{(s)})}{(ae_{k-1}^{(s)} + O(r_{-M_s}^2))(e_k^{(s)})} \\ &= \frac{e_k^{(s)}e_{k-1}^{(s)} + O(r_{-M_s}^3)}{e_k^{(s)}e_{k-1}^{(s)} + O(r_{-M_s}^3)} \\ &= \frac{r_{-M_s}^2 e^{2\pi i(k+(k-1))} + O(r_{-M_s}^3)}{r_{-M_s}^2 e^{2\pi i(k+(k-1))} + O(r_{-M_s}^3)} \\ &= 1 + O(r_{-M_s}). \end{aligned} \tag{4.1.7}$$

Taking logarithms we conclude that the nonzero entries of $\boldsymbol{\varepsilon}_s$ shrink at least as fast as $O(r_{-M_s}) < O(1/N_s^{\pi\sqrt{3}c_1})$ where $\pi\sqrt{3}c_1 > 1$. It should be noted that the number of non-zero elements is at most $2N_s$, so (4.1.2) gives

$$\|\boldsymbol{\varepsilon}_s\|_2 < O\left(\left((2N_s)\frac{1}{(N_s^{\pi\sqrt{3}c_1})^2}\right)^{(1/2)}\right) < O(1/N_s) \to 0. \tag{4.1.8}$$

Considering (4.1.6) and (4.1.8), we see that $\|\boldsymbol{A}_s^*\boldsymbol{W}_s^* - \boldsymbol{B}_s^*\|_\infty$ can be made

arbitrarily small by taking a large enough s. This says that F_s^* is approximately ν_s^*-conformal on each $\tau \in T_Z^{(s)}$, so in particular the PL-mapping $F_s^* \colon |T_Z^{(s)}| \to \mathbb{C}$ is now known to be an local homeomorphism. We note that (4.1.7) means that the boundary is mapped to a Jordan curve. Further F_s^* is homeomorphism by Lemma 2.2.1.

Step 5. Now we compare our Beltrami coefficients ν_s with the Beltrami coefficients of the secant map ν_s^*. We apply the algorithm by using average values

$$\nu_s|_{\tau_{j,k}} = \frac{\nu(Z_1) + \nu(Z_2) + \nu(Z_3)}{3} \tag{4.1.9}$$

for $\tau_{j,k} = (Z_1, Z_2, Z_3) \in T_Z^{(s)}$. We note that this differs from the value

$$\frac{\int_{\tau_{j,k}} \nu \, dx \, dy}{\text{area}(\tau_{j,k})}$$

by an amount which tends to zero with $O(1/N_s^2)$. Using the differentiability of ν, we can represent $\nu(Z_i)$ as $\nu(Z_0) + \nu_Z(Z_0)(Z_i - Z_0) + \nu_{\overline{Z}}(Z_0)\overline{(Z_i - Z_0)} + O(1/N_s^2)$, $i = 1, 2, 3$, where Z_0 is the barycenter of τ. Since (4.1.9), on $\tau_{j,k} = (Z_1, Z_2, Z_3) \in T_Z^{(s)}$ we have

$$\max_{j,k} \left| \nu_s|_{\tau_{j,k}} - \nu(Z_0) \right| = O(1/N_s^2)$$

as $s \to \infty$ and Z_0 always refers to the barycenter of $\tau_{j,k} \in T_Z^{(s)}$.

On the other hand,

$$W_i = F(Z_i) = F^*(Z_i) = W_0 + H_{a,b} \circ L_{\nu(Z_0)}(Z_i - Z_0) + O(1/N_s^2) \tag{4.1.10}$$

holds where $H_{a,b}$ and L_ν are defined in Section 2 and the constants a, b depend on Z_0. Recall that ν_s^* on $\tau_{j,k}$ is given by Corollary 2.1.4,

$$\nu_s^*|_{\tau_{j,k}} = -\frac{(Z_2 - Z_1)(W_3 - W_1) - (Z_3 - Z_1)(W_2 - W_1)}{(\overline{Z_2} - \overline{Z_1})(W_3 - W_1) - (\overline{Z_3} - \overline{Z_1})(W_2 - W_1)}.$$

Applying (2.1.4)–(2.1.5) in (4.1.10) and cancelling, we obtain

$$\begin{aligned}
& -\frac{(Z_2-Z_1)(W_3-W_1)-(Z_3-Z_1)(W_2-W_1)}{(\overline{Z_2}-\overline{Z_1})(W_3-W_1)-(\overline{Z_3}-\overline{Z_1})(W_2-W_1)} \\
= \; & -((Z_2-Z_1)(H_{a,0}\circ L_{\nu(Z_0)}(Z_3-Z_1)) \\
& \quad -(Z_3-Z_1)(H_{a,0}\circ L_{\nu(Z_0)}(Z_2-Z_1))+O(1/N_s^3))/ \\
& ((\overline{Z_2}-\overline{Z_1})(H_{a,0}\circ L_{\nu(Z_0)}(Z_3-Z_1)) \\
& \quad -(\overline{Z_3}-\overline{Z_1})(H_{a,0}\circ L_{\nu(Z_0)}(Z_2-Z_1))+O(1/N_s^3)) \\
= \; & -\frac{(Z_2-Z_1)(L_{\nu(Z_0)}(Z_3-Z_1))-(Z_3-Z_1)(L_{\nu(Z_0)}(Z_2-Z_1))}{(\overline{Z_2}-\overline{Z_1})(L_{\nu(Z_0)}(Z_3-Z_1))-(\overline{Z_3}-\overline{Z_1})(L_{\nu(Z_0)}(Z_2-Z_1))} \\
& +O(1/N_s) \\
= \; & -(Z_2-Z_1)((Z_3-Z_1)+\nu(Z_0)(\overline{Z_3}-\overline{Z_1})) \\
& \quad -(Z_3-Z_1)((Z_2-Z_1)+\nu(Z_0)(\overline{Z_2}-\overline{Z_1}))/ \\
& ((\overline{Z_2}-\overline{Z_1})((Z_3-Z_1)+\nu(Z_0)(\overline{Z_3}-\overline{Z_1}))- \\
& \quad (\overline{Z_3}-\overline{Z_1})((Z_2-Z_1)+\nu(Z_0)(\overline{Z_2}-\overline{Z_1})) \\
& +O(1/N_s) \\
= \; & \nu(Z_0)+O(1/N_s).
\end{aligned}$$

We conclude that

$$\max_{j,k}\left|\nu_s^*|_{\tau_{j,k}}-\nu_s|_{\tau_{j,k}}\right|=O\left(\frac{1}{N_s}\right). \tag{4.1.11}$$

Step 6. In this step we will prove:

$$\|\boldsymbol{W}_s^*\|_\infty=O(\log N_s)\text{ as }s\to\infty. \tag{4.1.12}$$

The support $|T_Z^{(s)}|$ of the triangulation in the logarithmic coordinates is a rectangle of width $R_{M_s}\approx\log N_s$ and height 2π. We may think of the image by F as a Riemann surface extended over a region of the W-plane. This image is a possibly non-schlicht topological quadrilateral whose "vertical" sides are the lifting of the small ellipse together with its reflection in the imaginary axis. The "horizontal" sides are two curves shifted from one another by $2\pi i$. If the condition (4.1.12) were false, this quadrilateral would contain points $W_{j,k}^{(s)}$

such that $\rho_s := |W_{j,k}^{(s)}|/\log N_s \to \infty$. Note that $W_{j,k} = F(Z_{j,k})$. This would imply that all curves joining the two vertical sides have Euclidean length at least $\rho_s \log N_s$. It follows from Lemma M, that the conformal module of this quadrilateral must also grow at least as fast as $\rho_s \log N_s$. Since $|T_Z^{(s)}|$ has conformal module $O(\log N_s)$, the quasiconformal mappings F must have arbitrarily large maximal dilatation; i.e., their Beltrami coefficent must have absolute value greater 1 at some point. This contradicts the fact that the Beltrami coefficent is ν, which is less than 1. Therefore (4.1.12) holds as claimed.

Step 7. The following notations will be used:

$$|\boldsymbol{A}_s^* - \boldsymbol{A}_s| := \sup |(\boldsymbol{A}_s^*)_{jk} - (\boldsymbol{A}_s)_{jk}|, \tag{4.1.13}$$

$$|\boldsymbol{B}_s^* - \boldsymbol{B}_s| := \sup |(\boldsymbol{B}_s^*)_k - (\boldsymbol{B}_s)_k|. \tag{4.1.14}$$

All elements of $(\boldsymbol{A}_s, \boldsymbol{B}_s)$ and $(\boldsymbol{A}_s^*, \boldsymbol{B}_s^*)$ in the same positions are equivalent formulas by ν_s and ν_s^* respectively. Considering Corollary 2.1.3, elements in $\boldsymbol{A}_s$, $\boldsymbol{A}_s^*$ resulting from triangle equations are given by $L_\nu(Z_i - Z_j)$, $L_{\nu^*}(Z_i - Z_j)$ respectively, where a given triangle is referred to by (Z_1, Z_2, Z_3) as in (4.1.9), and ν, ν^* refer to the constant values assigned to that particular triangle.

The elements satisfy

$$\begin{aligned} L_{\nu_s}(Z_i - Z_j) - L_{\nu_s^*}(Z_i - Z_j) &= \frac{2(\nu_s^* - \nu_s)\mathrm{Im}\ (Z_i - Z_j)}{(1+\nu_s)(1+\nu_s^*)} \\ &= O\left(\frac{1}{N_s^2}\right) \end{aligned}$$

by (4.1.11), because $|\nu|$ is bounded away from 1. The elements of $\boldsymbol{A}_s, \boldsymbol{A}_s^*$ from boundary equations do not depend on ν_s, ν_s^*, because right hand side is 0. We arrive at

$$|\boldsymbol{A}_s^* - \boldsymbol{A}_s| = O(1/N_s^2), \quad |\boldsymbol{B}_s^* - \boldsymbol{B}_s| = O(1/N_s), \tag{4.1.15}$$

the latter estimate resulting from a simple calculation based on (3.2.17).

Step 8. Using (4.1.6), we observe

$$\begin{aligned}\|\boldsymbol{A}_s\boldsymbol{W}_s^* - \boldsymbol{B}_s\|_2 &\leq \|\boldsymbol{A}_s\boldsymbol{W}_s^* - \boldsymbol{A}_s^*\boldsymbol{W}_s^*\|_2 + \|\boldsymbol{A}_s^*\boldsymbol{W}_s^* - \boldsymbol{B}_s^*\|_2 \\ &\quad + \|\boldsymbol{B}_s^* - \boldsymbol{B}_s\|_2 \\ &= \|(\boldsymbol{A}_s - \boldsymbol{A}_s^*)\boldsymbol{W}_s^*\|_2 + \|\boldsymbol{\varepsilon}_s\|_2 + \|\boldsymbol{B}_s^* - \boldsymbol{B}_s\|_2.\end{aligned}$$

Considering the construction of the associated linear systems, each row of $\boldsymbol{A}_s$ or $\boldsymbol{A}_s^*$ contains at most three non-zero entries, as only three variables appear in the linear equations. The entries of $(\boldsymbol{A}_s - \boldsymbol{A}_s^*)\boldsymbol{W}_s^*$ are of the form $\sum_p (A_{p(j,k),k} - A^*_{p(j,k),k})W_{p(j,k)}$, where the map $p : \{(j,k)\} \to \{1 \leq p \leq n_v\}$ is a bijection, at most three of the summands are nonzero. Thus $\|(\boldsymbol{A}_s - \boldsymbol{A}_s^*)\boldsymbol{W}_s^*\|_\infty \leq 3|\boldsymbol{A}_s - \boldsymbol{A}_s^*|\,\|\boldsymbol{W}_s^*\|_\infty = O(\log N_s/N_s^2)$ by (4.1.12) and (4.1.15). This vector has n_e elements, so we may estimate its L_2-norm,

$$\begin{aligned}\|(\boldsymbol{A}_s - \boldsymbol{A}_s^*)\boldsymbol{W}_s^*\|_2 &\leq O\left(\left(n_e(\frac{\log N_s}{N_s^2})^2\right)^{1/2}\right) \\ &= O\left(\left(N_s^2 \log N_s \frac{(\log N_s)^2}{N_s^4}\right)^{1/2}\right) \\ &= O\left((\log N_s)^{3/2}/N_s\right).\end{aligned}$$

By a similar calculation, we obtain

$$\begin{aligned}\|\boldsymbol{B}_s^* - \boldsymbol{B}_s\|_2 &\leq O\left(\left(\mathrm{N_s}(\frac{1}{N_s})^2\right)^{1/2}\right) \\ &= O(1/N_s^{1/2}).\end{aligned}$$

Further we have

$$\|\boldsymbol{R}_s\|_\infty < \|\boldsymbol{R}_s\|_2 = \|\boldsymbol{A}_s\boldsymbol{W}_s - \boldsymbol{B}_s\|_2 \leq \|\boldsymbol{A}_s\boldsymbol{W}_s^* - \boldsymbol{B}_s\|_2$$

by minimality of $\|\boldsymbol{A}_s\boldsymbol{W}_s - \boldsymbol{B}_s\|_2 = \|\boldsymbol{R}_s\|_2$ (recall (4.1.16) and (4.1.8)). There-

fore we have proved that

$$\|\boldsymbol{R}_s\|_\infty = \|\boldsymbol{A}_s\boldsymbol{W}_s - \boldsymbol{B}_s\|_\infty \to 0. \tag{4.1.16}$$

This means that the Beltrami coefficient of F_s is approximately ν_s on each $\tau \in T_z^{(s)}$. Hence F_s is also a local homeomorphism and has the Beltrami coefficients close to ν_s^*. Let ν_s' be the Beltrami coefficients of PL mappings which is induced by $\{Z_{j,k}^{(s)}\}$ and $\{W_{j,k}^{(s)}\}$. We note that (4.1.16) means

$$\max_{j,k} \left| \nu_s' \,|_{j,k} - \nu_s^*|_{j,k} \right| \to 0 \tag{4.1.17}$$

as $s \to \infty$.

Step 9. By (4.1.5) and (4.1.6), we obtain

$$\begin{aligned} \|\boldsymbol{A}_s(\boldsymbol{W}_s - \boldsymbol{W}_s^*)\|_\infty &\leq \|\boldsymbol{A}_s\boldsymbol{W}_s - \boldsymbol{B}_s\|_\infty + \|\boldsymbol{B}_s - \boldsymbol{B}_s^*\|_\infty + \|\boldsymbol{B}_s^* - \boldsymbol{A}_s^*\boldsymbol{W}_s^*\|_\infty \\ &\quad + \|\boldsymbol{A}_s^*\boldsymbol{W}_s^* - \boldsymbol{A}_s\boldsymbol{W}_s^*\|_\infty \\ &= \|\boldsymbol{R}_s\|_\infty + \|\boldsymbol{B}_s^* - \boldsymbol{B}_s\|_\infty + \|\boldsymbol{\varepsilon}_s\|_\infty \\ &\quad + \|(\boldsymbol{A}_s^* - \boldsymbol{A}_s)\boldsymbol{W}_s^*\|_\infty. \end{aligned} \tag{4.1.18}$$

Hence we may conclude that $\|\boldsymbol{A}_s(\boldsymbol{W}_s - \boldsymbol{W}_s^*)\|_\infty \to 0$.

Now we will prove: If $\{\boldsymbol{X}_s\} \in \mathbb{C}^{n_v}$ is such that $\boldsymbol{A}_s\boldsymbol{X}_s \to 0$, then $\boldsymbol{X}_s \to 0$. Consider a subsequence of $\{\boldsymbol{X}_s\}$ which converges to a limit $\boldsymbol{X}$. By the continuity we have $\boldsymbol{A}_s\boldsymbol{X}_s \to 0$ and hence $\boldsymbol{X} = 0$ by Lemma 3.4.1. Thus we see that every convergent subsequence of $\{\boldsymbol{X}_s\}$ converges to 0. If $\{\boldsymbol{X}_s\}$ is bounded, then it indeed has a convergent subsequence, so it follows that $\boldsymbol{X}_s \to 0$ as desired.

Next we assume that $\{\boldsymbol{X}_s\}$ is not bounded. The maximum absolute value $|X_p^{(s)}|$ of an element of $\{\boldsymbol{X}_s\}$ occurs infinitely often for some fixed index p_0. On the corresponding subsequence we have $|X_{p_0}^{(s)}| \to \infty$. Let

$$\boldsymbol{Y}_s = \frac{1}{X_{p_0}^{(s)}}\boldsymbol{X}_s,$$

so $|\boldsymbol{Y}_s| = 1$. Also

$$\boldsymbol{A}_s \boldsymbol{Y}_s = \frac{1}{X_{p_0}^{(s)}} \boldsymbol{A}\boldsymbol{X}_s \to 0$$

on the subsequence, where $|X_{p_0}^{(s)}| > 1$ for large n. Since $\{\boldsymbol{Y}_s\}$ is bounded, by the previous paragraph $\boldsymbol{Y}_s \to 0$, which contradicts $|\boldsymbol{Y}_s| = 1$. Therefore this case does not occur.

Considering $\|\boldsymbol{A}_s(\boldsymbol{W}_s - \boldsymbol{W}_s^*)\|_\infty \to 0$, we obtain that

$$\|\boldsymbol{W}_s - \boldsymbol{W}_s^*\|_\infty \to 0 \tag{4.1.19}$$

as $s \to \infty$. This says that the points $\boldsymbol{W}_s$ produced by the algorithm differ by an arbitrarily small amount from the image vertices under the true ν-conformal mapping F.

Step 10. Finally, we apply the exponential mapping via (3.2.1) and (3.2.2) to obtain the sequence of PL-mappings $f_s \in PL(|T_z^{(s)}|)$ which send each 2-simplices $(z_1, z_2, z_3) \in T_z^{(s)}$ to the 2-simplices (w_1, w_2, w_3) where $w_j := \exp \circ F_s \circ \log(z_j)$. Note that the domain $\{|T_z^{(s)}|\}$ exhausts the unit disk $\mathbb{D}$, produced by the algorithm for meshes determined by (M_s, N_s).

Let f_s^* be the secant map which is induced by f and $T_z^{(s)}$, and let μ_s^* be the Beltrami coefficients of f_s^*. We note that

$$f_s^*(z_{j,k}) = \exp \circ F_s^* \circ \log(z_{j,k}) = \exp \circ F_s^*(Z_{j,k}) = e^{W_{j,k}^*}.$$

Considering the Beltrami coefficients of f_s^* and Lemma 2.2.1, we see that f_s^* is a quasiconformal mapping if s is large enough. Further the images under quasiconformal mapping $\{f_s^*(|T_z^{(s)}|)\}$ exhaust the unit disk $\mathbb{D}$. Considering Lemma J, we conclude that f_s^* converges to the true solution f locally uniformly on $\mathbb{D}$. Hence f_s is also a quasiconformal mapping if s is large enough, and $f_s \to f$ locally uniformly on $\mathbb{D}$. □

Chapter 5

Numerical experiments

In this chapter, we will present numerical experiments of our algorithm for some constructive examples. We have calculated with machine precision in Mathematica on a Macintosh platform (3.33 GHz CPU, 16.00 G RAM) for all experiments. The *Mathematica* routine `LeastSquares` handles sparse matrices [5, 37], a data structure which registers only the nonzero entries appearing in a matrix or vector. Further examples are presented in the appendix with the error of the Beltrami coefficients.

5.1 Comparison with true solution

In the first several examples we compare the results produced by our algorithm with an exact formula for the quasiconformal mapping under consideration.

5.1.1 Constant Beltrami coefficient

We consider the case that the Beltrami coefficient is constant $\mu(z) = c$. First we note that the real-linear mapping L_μ maps the unit circle to an ellipse with semi-axes 1, $(1 - |\mu|)/(1 + |\mu|)$ slanted in the directions $(1/2)\arg\mu$, $(1/2)(\arg\mu + \pi)$ respectively, modulo π. Let f be the conformal mapping to $\mathbb{D}$ from an ellipse $E_{a,b}$ with semi-major and semi-minor axes of lengths a, b $(a^2 - b^2 = 1)$ and foci at ± 1. It was presented in [36] that f has the following

form:

$$f(z) = \sqrt{k}\,\mathrm{sn}\,(\frac{2K}{\pi}\sin^{-1}u; k^2) \tag{5.1.1}$$

where the Jacobi elliptic function modulus k is related to the complete elliptic integral K and the Jacobi theta functions by the formulas

$$q = (a+b)^{-4} = e^{-\pi K(1-m)/K(m)},$$

$$k = \sqrt{m} = \left(\frac{\theta_2}{\theta_3}\right)^2,$$

with notation from [40].

The ellipse $E_{a,b}$ is sent by the conformal linear mapping $H_{1/(2\sqrt{\mu}),0}$ to the ellipse $E'_{a,b}$ with semi-axes a, b. Then via (5.1.1) this is transformed conformally to the unit disk.

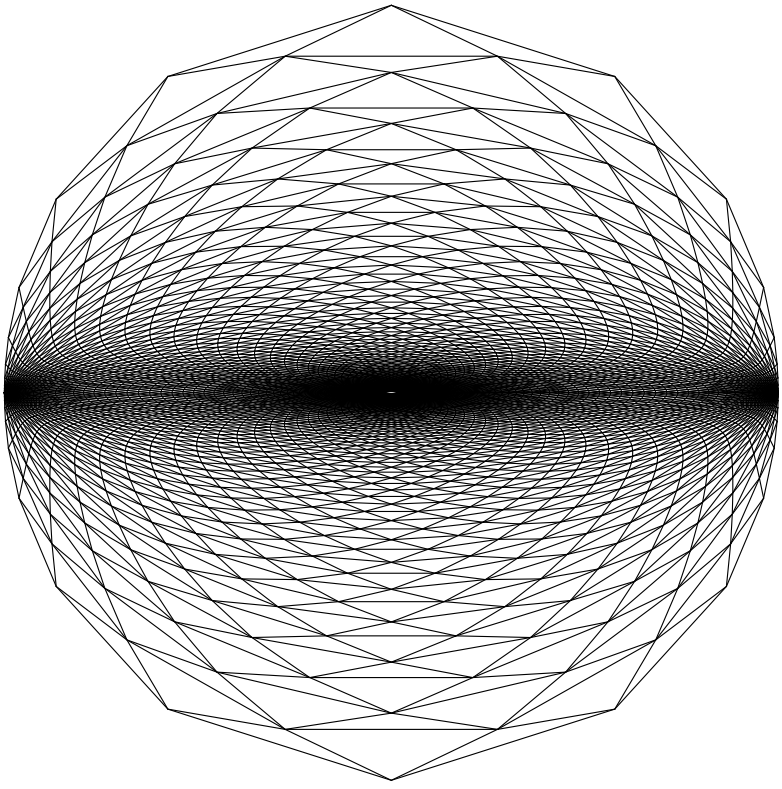

Figure 5.1.1: Image for constant Beltrami derivative $\mu = 0.5$ and $(M, N) = (52, 64)$. Observe the "crowding phenomenon" near the boundary.

It is well known that a conformal mapping from an ellipse to a disk tends to "crowd" boundary points near the images of the endpoints of the major axis. The crowding, or maximum ratio of separation of N points sent to the Nth roots of unity, increases exponentially as a function of the aspect ratio a/b [11, section 2.6]. In contrast, the affine mapping L_μ which we combined with this conformal mapping produces little crowding. The combined effect is a great deal of crowding near $w = 1$, as it can be perceived in Figure 5.1.1.

Simply we chose the constant c as $\mu = 0.1,\ 0.3,\ 0.5,\ 0.7$ and applied our algorithm for the basic meshes defined by $N = 16, 32, 48, \ldots 256$, with $M = (N\lceil \log N \rceil)/2$ where $\lceil \cdot \rceil$ is the ceiling function. In this case $c_1 N \log N < M$ hold in the view of (4.1.1). The list of number of equations and variables with the calculating time for constructing the matrix time and solving the least squares problems are presented in Table 5.1.1. Table 5.1.2 presents the maximum error over all w_{kj} when these points are compared to the images of z_{kj} under the exact quasiconformal mapping described in the preceding paragraph. As is to be expected, the error increases when the Beltrami derivative increases. However the error decreases when N is increased. It was found that for $\mu = 0.7$ and a rather coarse mesh such as $(M, N) = (36, 48)$, the image of T_{MN} is not a triangulation, inasmuch as a few of the w-triangles near ± 1 are improperly oriented. In spite of this fact, the values obtained for the conformal mapping are not very far off.

	16	32	48	64	80	96	112	128
Constructing	0.51	1.27	3.01	7.06	11.60	18.00	24.98	33.87
Solving	0.03	0.26	0.64	1.59	2.80	4.24	6.12	8.47

Table 5.1.1: The maximum of the calculating time for constructing the equations and solving the least squares problems for constant Beltrami coefficient and $N = 16, 32, 48, 64, 80, 96, 112, 128$ with $M = (N\lceil \log N \rceil)/2$. Values are in seconds.

We analyze the variation of the error as a function of the radius for the case $\mu = 0.3$. Figure 5.1.2 shows the maximum error over k in the calculated value of w_{jk} for each fixed j. It is seen that the error remains approximately constant for $r < 0.7$ and then increases rather sharply for $0.7 < r < 1$.

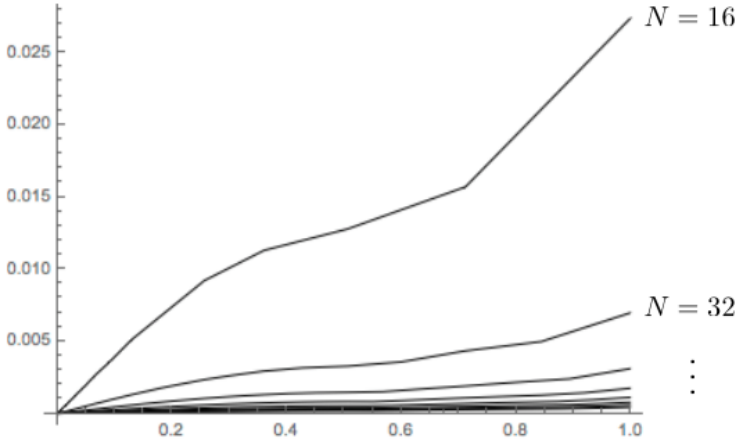

Figure 5.1.2: Numerical errors of the algorithm for different values of (M, N) with $\mu = 0.3$. The horizontal axis indicates the distance $r_j = |z_{jk}|$ of the z-points from the origin; the vertical axis gives the maximum discrepancy (over k) of the calculated value of w_{jk} from the true value.

Thus the maximum values in Table 5.1.2 are much higher than the average errors. As noted above, the maximum error, which occurs on the boundary, decreases as a function of N.

	16	32	48	64	80	96	112	128
0.1	0.012	0.0031	0.0014	0.00077	0.0005	0.00034	0.00025	0.00019
0.3	0.027	0.0070	0.0031	0.0018	0.0011	0.00078	0.00057	0.00044
0.5	0.061	0.020	0.011	0.0065	0.0042	0.0030	0.0022	0.0017
0.7	0.244	0.120	0.086	0.063	0.045	0.034	0.026	0.021

Table 5.1.2: The maximum of the absolute errors between the solutions by our algorithm and the approximation of real values of constant Beltrami coefficients $\mu = 0.1, 0.3, 0.5, 0.7$ and $N = 16, 32, 48, 64, 80, 96, 112, 128$ with $M = (N\lceil \log N \rceil)/2$.

5.1.2 Radial quasiconformal mappings

Let $\varphi\colon [0,1] \to [0,1]$ be an strictly increasing diffeomorphism of the unit interval. We define the radially symmetric function as

$$f(z) = \varphi(|z|)e^{i\arg z} = \varphi(|z|)\frac{z}{|z|}. \tag{5.1.2}$$

The function f has Beltrami derivative equal to

$$\mu(z) = \frac{|z|\varphi'(z)/\varphi(z) - 1}{|z|\varphi'(z)/\varphi(z) + 1}\frac{z}{\overline{z}} \tag{5.1.3}$$

when $z \neq 0$. As an illustration we will take

$$\varphi(r) = (1 - \cos 3r)/(1 - \cos 3)$$

in Figure 5.1.3. In this case the essential supremum of the Beltrami coefficient is $\|\mu\|_\infty \approx 0.65$.

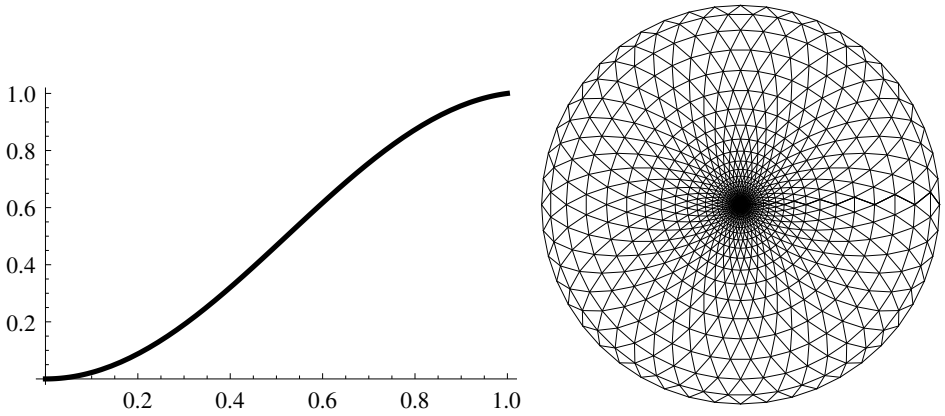

Figure 5.1.3: Radial function φ (left), together with the induced rotationally symmetric image domain.

The domain points z_{jk} on the real axis were selected, and the values of w_{jk} produced by the algorithm were compared with the true values $\varphi(|z_{jk}|)$. The results are given in Table 5.1.3. It was also observed that as in the previous example, the errors increase as the radius increases.

	16	32	48	64	80	96	112	128
Error	0.040	0.014	0.0058	0.0034	0.0021	0.0015	0.0011	0.00086

Table 5.1.3: Maximum absolute error for radially symmetric quasiconformal mapping defined by (5.1.3).

	16	32	48	64	80	96	112	128
Error	0.067	0.036	0.025	0.019	0.015	0.013	0.011	0.010

Table 5.1.4: Maximum absolute error $|\psi(\theta) - f(e^{i\theta})|$ for μ defined by (5.1.5).

5.1.3 Sectorial quasiconformal mappings

In a similar spirit, we let $\psi\colon [0, 2\pi] \to [0, 2\pi]$ be an increasing diffeomorphism. Write $\widetilde{\psi}(e^{i\theta}) = e^{i\psi(\theta)}$. Then the sectorially symmetric function

$$f(z) = |z|\,\widetilde{\psi}\left(\frac{z}{|z|}\right) \tag{5.1.4}$$

has Beltrami derivative equal to

$$\mu(z) = \frac{1 - \psi'(\theta)}{1 + \psi'(\theta)}\,\frac{z}{\overline{z}} \tag{5.1.5}$$

when $z \neq 0$. As an example we will take

$$\psi(\theta) = \begin{cases} \frac{\theta}{2}, & 0 \leq \theta \leq \pi, \\ \frac{\pi}{2} + \frac{3(\theta-\pi)}{2}, & \pi \leq \theta \leq 2\pi. \end{cases}$$

as in Figure 5.1.4. In this example μ does not satisfy the hypothesis of Theorem 4.1.1 because it is not continuous. The arguments of the final boundary values on the unit circle were compared with the true values $\psi(\theta)$; see Table 5.1.4.

5.2 Trivial Beltrami coefficients

Let $\mu \in L^\infty(\mathbb{D})$ with $\|\mu\|_\infty < 1$. If the corresponding normalized solution f^μ satisfies $f^\mu(z) = z$ on the unit circle, μ called a trivial Beltrami coef-

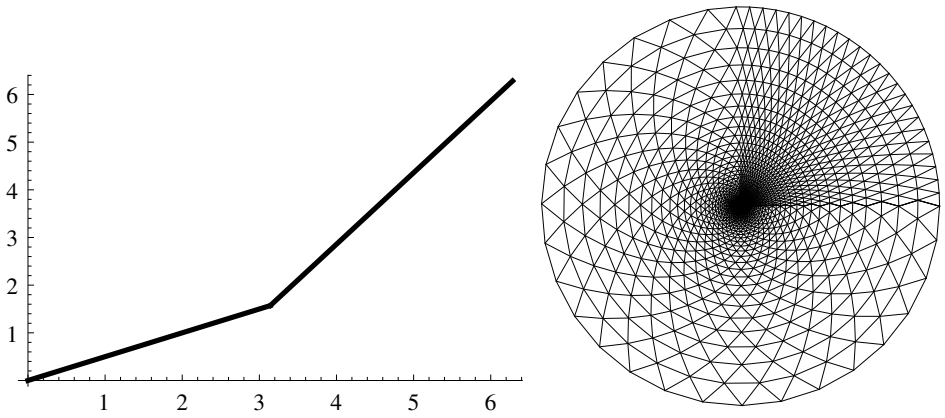

Figure 5.1.4: Angular function ψ (left), together with image domain under the sectorial mapping (5.1.4).

ficient. Trivial Beltrami coefficients play an important role in the theory of Teichmüller space. Sugawa [35] showed a criterion for the triviality of the Beltrami coefficients, and gave an example for a trivial Beltrami coefficient. Let N be a non-negative integer and $a_j(t)$ $(1 \leq j \leq N)$ be essentially bounded measurable functions in $t \geq 0$ so that

$$\mu(z) := \sum_{j=0}^{N} a_j \left(-\log|z|\right) \left(\frac{z}{|z|}\right)^{j+2}$$

satisfies $\|\mu\|_\infty < 1$. Then his results implies that μ is a trivial Beltrami coefficient. For the experiment, we chose

$$a_j(z) := \frac{2}{3}\left(\frac{\sin 10z}{2}\right)^{j+1}.$$

We show our result in Figure 5.2.1. Further the error between the boundary and the identity values, and the error of the Beltrami coefficients are plotted in Figure 5.2.2. It was observed that the error at the boundary values are bounded by 0.0032 (the distance between the vertices is 0.05).

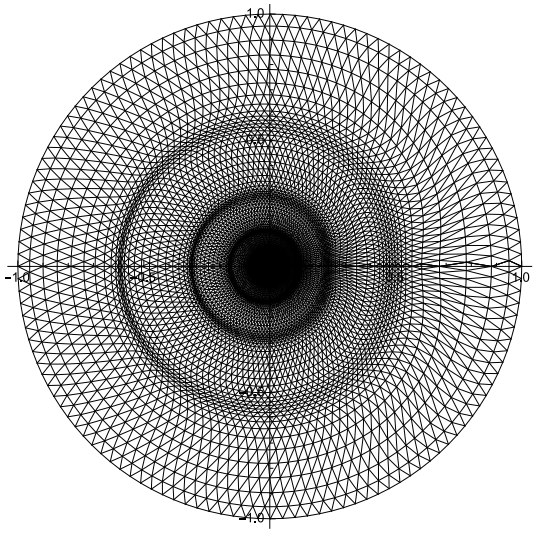

Figure 5.2.1: The result made by our algorithm with trivial coefficient μ_1.

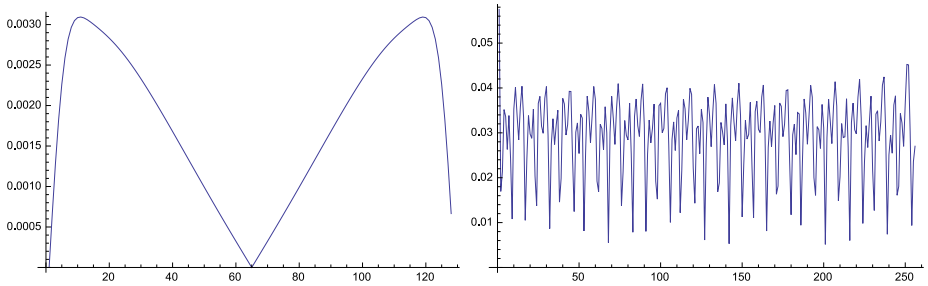

Figure 5.2.2: The errors of the boundary values (left), the difference between the induced Beltrami coefficients to μ_1 (right).

5.3 Comparison with Daripa's method

We will compare our algorithm with Daripa's method. Daripa [7] has calculated quasiconformal mappings from $\mathbb{D}$ to the exterior of an ellipse (the origin being sent to ∞) which has following Beltrami coefficients:

$$\begin{aligned} \mu_1(z) &= |z|^2 e^{0.65(iz^5-2.0)}, \\ \mu_2(z) &= \frac{1}{2}|z|^2 \sin(5\mathrm{Re}\ z). \end{aligned}$$

Let $h(z)$ be the rational function of the form:

$$h(z) = \frac{(1+\alpha) - (1-\alpha)z^2}{2\alpha z}.$$

The rational function h maps $\mathbb{D}$ conformally to the exterior of an ellipse with aspect ratio α. Further let f^{μ_1} and f^{μ_2} be the normalized quasiconformal self-mapping of the unit disk which has Beltrami coefficients μ_1, μ_2 respectively. The composition $h \circ f^{\mu_j}$ are μ_j-conformal mappings to the exterior of the ellipse ($j = 1, 2$).

In the examples in [7], $\alpha = 0.6$ was chosen. However, the inner ellipses in [7] appear to have aspect ratios of approximately 0.47; axes are not drawn. We made adjustments for the fact that Daripa uses M radii equally spaced in $[0, 1]$, in contrast to the exponential spacing we have been using. We show an result $(M, N) = (64, 64)$ in Figure 5.3.1 for comparison. Our image looks like similar to Daripa's images in [7].

Computation times are reported in [7] for $N = 64$ as approximately 8.5 seconds of CPU on a MIPS computer described as "approximately 15 times slower than the CRAY-YMP at Texas A & M University" of that time. Our CPU times were approximately 3.17 seconds for the first example and 3.16 seconds for the other.

It is apparent from the examples in [7] that Beltrami derivatives with a great deal of oscillation were used in order to create an interesting problem. Figure 5.3.2 shows our results for the mapping of the disk to the exterior of

the same ellipse, with Beltrami derivative

$$\mu(z) = 0.9 \sin |20z| \tag{5.3.1}$$

and $(M, N) = (128, 128)$.

In the above examples which we have taken from [7], μ satisfies $\|\mu\|_\infty \approx 0.5$. However it should be noted that μ satisfies $|\mu(z)| < 0.12$ for $|z| < 0.5$, and $|\mu(z)| < 0.12$ for $|z| < 0.3$. In fact, an important limitation stated in [7] is that the Beltrami coefficient μ must be Hölder continuous. Further, it is recommended that μ vanishes at least as fast as $|z|^3$ at the origin for the method to work properly. In [12] it is similarly recognized that the computation time increases as $\|\mu\|_\infty$ increases. Our algorithm, in contrast, is not subject to any such requirement on μ.

Daripa's main algorithm requires an evaluation of the $\partial/\partial\overline{z}$ derivatives which appear in the singular integrals. The operation count of one iteration of Daripa's method is $O(MN \log N)$. This should be multiplied by the average number of iterations required, which depends on how refined the mesh is and how much accuracy is desired.

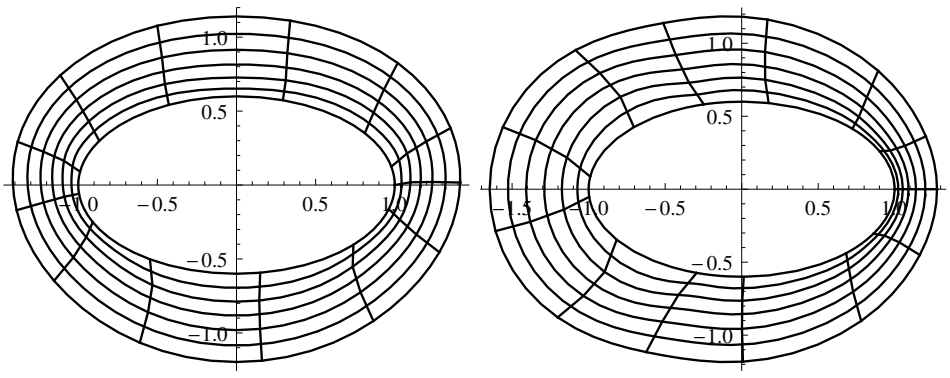

Figure 5.3.1: The quasiconformal self-mappings of unit disk with Beltrami derivatives μ_1 (left), μ_2 (right) followed by a conformal mapping to exterior of an ellipse as in [7].

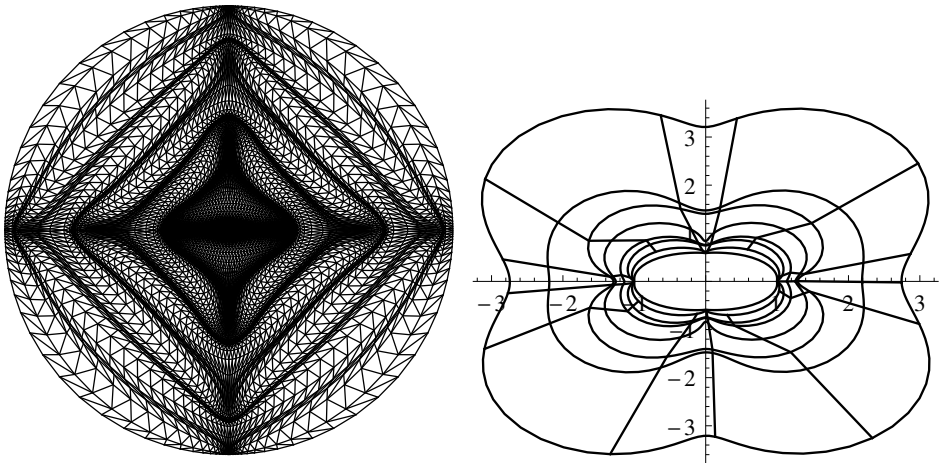

Figure 5.3.2: Quasiconformal mappings to the unit disk (left) and the exterior of an ellipse (right) determined by (5.3.1).

5.4 Computational cost

In this section we will estimate computational cost of our algorithm. As described in Chapter 3, we use a linear system $(\boldsymbol{A}, \boldsymbol{B})$. For a fixed dimensions M, N for our basic mesh, the matrices $\boldsymbol{A}, \boldsymbol{B}$ are of orders $n_e \times n_{\mathrm{v}}$, $n_{\mathrm{e}} \times 1$ respectively (recall that $n_{\mathrm{e}} = 4MN+2(N-1)+1$ and $n_{\mathrm{v}} = (2M+1)N$). The total number of elements contained in $\boldsymbol{A}$ is $O(M^2N^2)$. However, we noted in the proof of Theorem 4.1.1 that the number of nonzero elements of any row of A is no greater than 3. Further the number of nonzero elements of any column of $\boldsymbol{A}$ is no greater than 7. It should be noted that each variable W_{jk} in (3.2.10), (3.2.12) corresponds to a vertex of at most six triangles; the only vertex appearing in seven equations is $W_{0,0}$, cf. (3.2.18). Hence the number of nonzero elements in $\boldsymbol{A}$ is no greater than $O(MN)$.

Recall that the linear system $\boldsymbol{AV} = \boldsymbol{B}$ is overdetermined and in general there is no exact solution. Hence we took the least squares solution as the approximation. There are many numerical methods available for the least squares problem (see a comprehensive reference [5] for details). For simplicity we discuss the method of "normal equations," that is, the solution of $\boldsymbol{A}^H\boldsymbol{AV} = \boldsymbol{A}^H\boldsymbol{B}$, where $\boldsymbol{A}^H$ is the conjugate transpose of $\boldsymbol{A}$. It is easily seen that by construction the columns of $\boldsymbol{A}$ are linearly independent, so that

$\boldsymbol{A}^H\boldsymbol{A}$ is positive definite, and each row or column of $\boldsymbol{A}^H\boldsymbol{A}$ contains at most 7 nonzero entries. These entries are not consecutive, but the index correspondence in (3.3.1) may be taken so that the row bandwidth of $\boldsymbol{A}^H\boldsymbol{A}$ is $2M$.

When one applies Gaussian reduction to $(\boldsymbol{A}, \boldsymbol{B})$, the n-th of the n_{v} rows will only need to reduce at most $2M$ of the succeeding rows, and will require no more than $2M$ floating-point multiplications for each one. Hence the total operation count is of the order of $O(n_{\mathrm{v}}(2M)^2) = O(M^3N)$. Once $\boldsymbol{A}^H\boldsymbol{A}$ has been thus reduced to echelon form, the computational cost of back substitution is seen to be no more than $O(M^2N)$. These computations do not require a significant amount of storage other than the original data.

In summary, when one doubles the mesh dimensions M, N, the memory requirement is at most multiplied by 4 (which is the same as the increase in the mesh itself) and the computation time by 16. Our numerical experiments indicate that the more sophisticated least squares algorithms found in packaged software appear to reduce these exponents slightly.

5.5 Future tasks

We think that our algorithm can be used for solving the Beltrami equation on the entire z-plane (normalized by fixing 0, 1, and ∞) instead of the unit disk. One simply eliminates the step of extending the Beltrami coefficient from the disk to its exterior by reflection. We have not yet investigated this question numerically. We conjectured that our algorithm will converge to the true μ-conformal mapping even when μ is piecewise smooth, and perhaps in even greater generality. The conjectured is suggested by the numerical examples in Chapter 5 and Appendix. The estimates in the proof of Theorem 4.1.1 concerning L^2 norms would not be greatly affected if only a small proportion of the terms in the sums failed to tend to zero as fast as required. We hope to look into these questions in the near future.

Appendix

For the interested readers we present several results of our numerical experiments. The left figure is the results by our algorithm. The right figure is the error of the Beltrami coefficient: the horizontal axis indicates the index from the origin, the vertical axis gives the maximum discrepancy (over k) of the calculated value of the Beltrami coefficient from the true value.

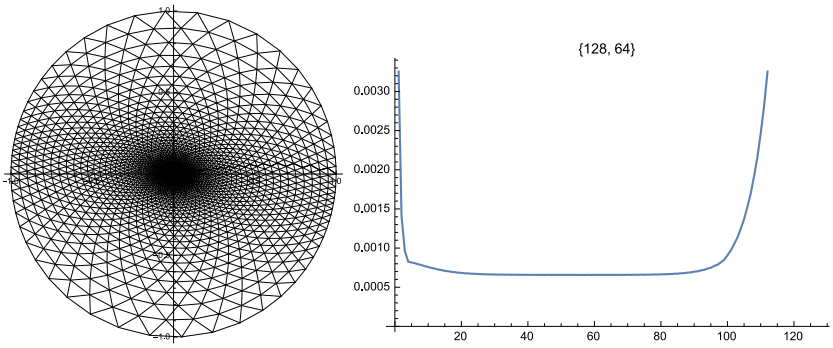

Figure 5.5.1: $\mu(z) = 0.15 - 0.15i$ $(M = 128, N = 64)$.

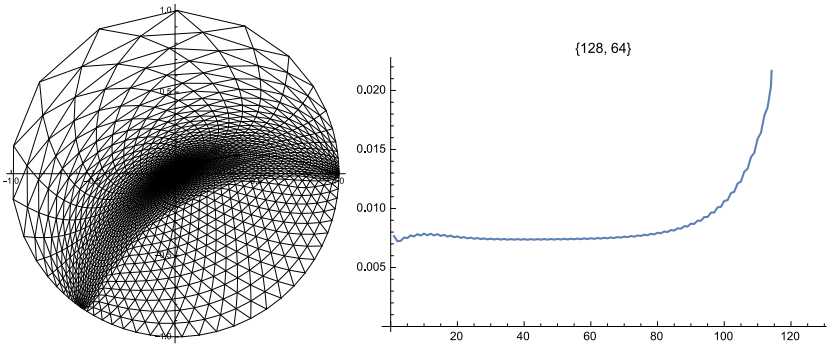

Figure 5.5.2: $\mu(z) = 1/2$ for $\{z \in \mathbb{D} : \text{Im } z > -1/3\}$, 0 for others ($M = 128, N = 64$). Note that μ is not continuous on $\{z \in \mathbb{D} : \text{Im } z = -1/3\}$.

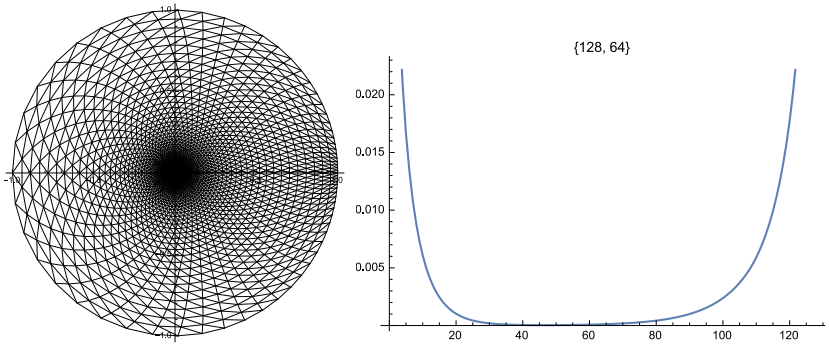

Figure 5.5.3: $\mu(z) = z/2$ ($M = 128, N = 64$).

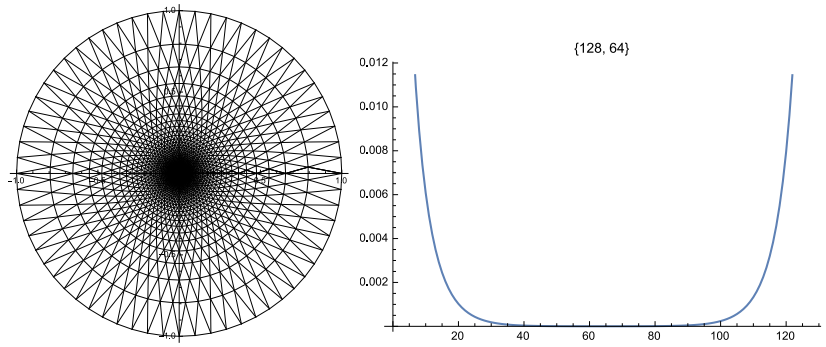

Figure 5.5.4: $\mu(z) = z^2/2$ ($M = 128, N = 64$).

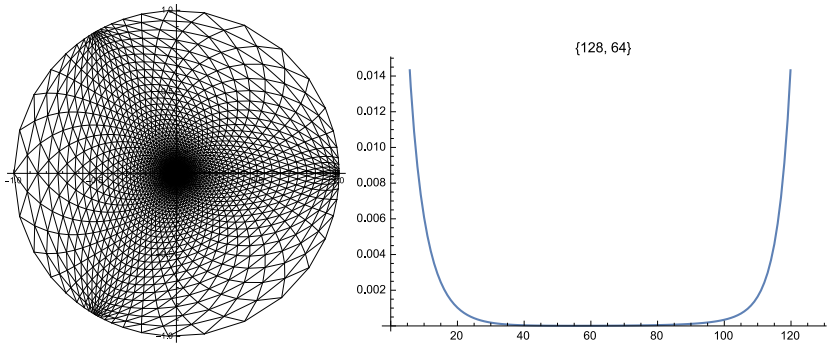

Figure 5.5.5: $\mu(z) = \overline{z}/2$ $(M = 128, N = 64)$.

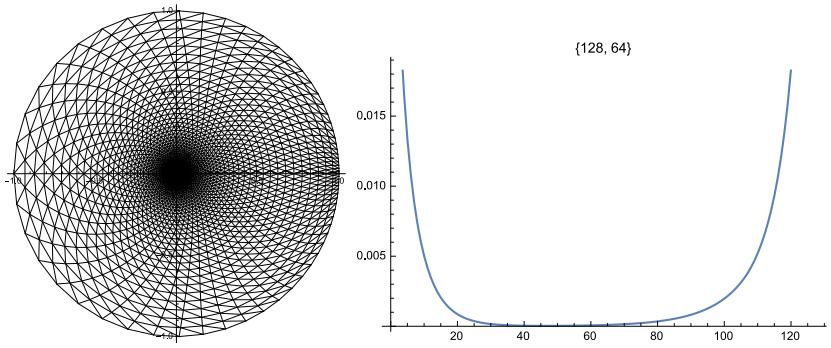

Figure 5.5.6: $\mu(z) = \sin(z)/2$ $(M = 128, N = 64)$.

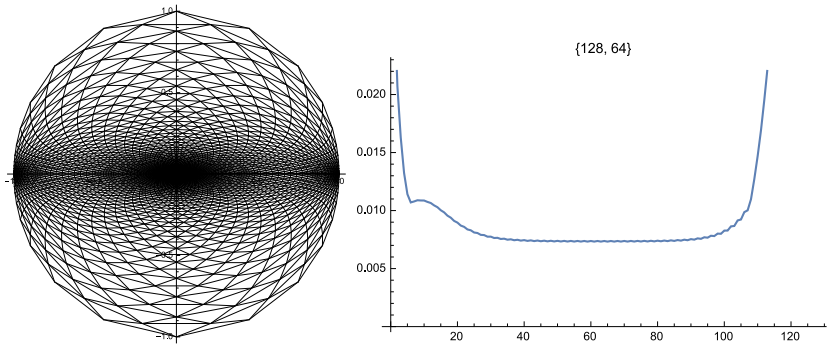

Figure 5.5.7: $\mu(z) = \cos(z)/2$ $(M = 128, N = 64)$.

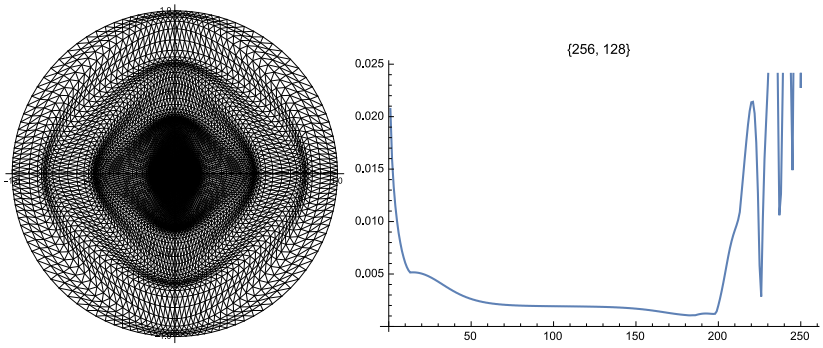

Figure 5.5.8: $\mu(z) = \cos(20|z|)/2$ $(M = 256, N = 128)$.

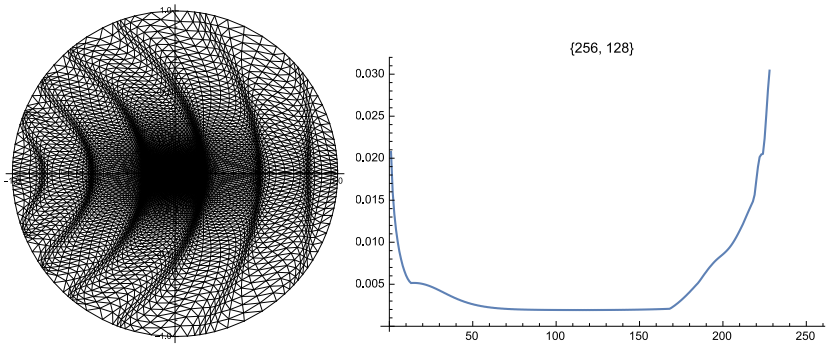

Figure 5.5.9: $\mu(z) = \cos(20|z| + \pi/2)/2$ $(M = 256, N = 128)$.

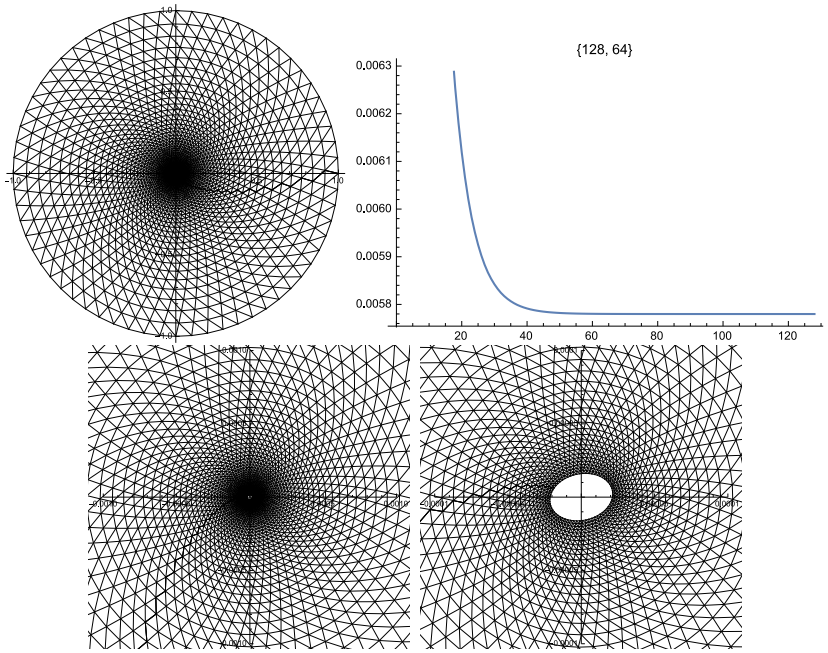

Figure 5.5.10: $\mu(x+iy) = \frac{(1+6i)x-(6-i)y}{37x-37iy}$ $(M = 128, N = 64)$. This is the Beltrami coefficent of a logarithmic spiral map $f^{\mu}(z) = z|z|^{i/6}$.

Notations

We summarize the notations.

Symbol	Definition
$\mathbb{C}$	the complex plane
$\widehat{\mathbb{C}}$	the Riemann sphere
$C^k(D)$	the set of functions which are in the class C^k on the domain $D \subset \mathbb{C}$
$\mathbb{D}$	the unit disk $\{z \in \mathbb{C} : \lvert z\rvert < 1\}$.
f^μ	the quasiconformal mapping which has the Beltrami coefficient μ
Int X	the interior of a domain $X \subset \mathbb{C}$
$\boldsymbol{M}_{m,n}(\mathbb{C})$	the set of complex (m,n)-matrixes for positive fingers m, n
μ_f	the Beltrami coefficient of f, i.e. $\mu(z) = f_{\overline{z}}/f_z$
$PL(T)$	the set of continuous functions which is linear on each 2-simplices in the triangulation T
$\lvert T\rvert$	the union of all 2-simplicies of a triangulation T
$\lVert\cdot\rVert_\infty$	the essential supremum

Acknowledgements

First and foremost, I would like to expresses my sincere gratitude to my supervisor, Professor Dr. Toshiyuki Sugawa, for his many helpful advices, kind guidance and constant encouragement. I have learned a great deal from his mathematical and social sharp insights.

To Professor Dr. R. Michael Porter, I am grateful for his warm support, kind suggestions and great generosity. He introduced me to many effective mathematical programming techniques and interesting ideas. Also I would like to thank him and his family for their kind hospitality when I visited Querétaro. It was my great pleasure that I could work with him. I am also thankful to Professor Dr. Masahiko Taniguchi, Professor Dr. Yasushi Yamashita and Professor Dr. Hiroshi Yanagihara for their valuable comments and warm encouragements.

I would also like to thank Dr. Ikkei Hotta and Dr. Rintaro Ohno for many mathematical and private conversations. Further I would like to express my deep appreciation to the past and present members of the Sugawa Laboratory (Ms. Norie Gouke, Mr. Naoki Hiranuma, Dr. Yan Jiang, Ms. Mai Kodaka, Mr. Ryota Kurosaki, Ms. Ming Li, Ms. Lijie Sun, Dr. Li-Mei Wang and Dr. Tanran Zhang) and to the staffs of division of mathematics (Ms. Chisato Karino, Ms. Sumie Narasaka and Ms. Makiko Owase). Further I would like to thank all the other colleagues of the Institute for their kind support.

This research could not have been possible without the financial founding and research support of the IIARE, Tohoku University, and I would like to express my gratitude to the agency. Also I am grateful to Professor Yasuji Sawada for many discussions, valuable comments and warm encouragement. He was always able to motivate me further.

Last but not least, I am deeply indebted to my wife for her continued support and encouragement. I also would like to thank my family for their understanding.

Bibliography

[1] L. V. Ahlfors, *Lectures on quasiconformal mappings*, 2nd ed., University Lecture Series, **38**, Amer. Math. Soc., Providence, RI, (2006).

[2] L. V. Ahlfors, L. Bers, *Riemanns mapping theorem for variable metrics*, Ann. of Math. (2) **72** (1960), 385-404.

[3] K. Astala, T. Iwaniec, G. Martin, *Elliptic Partial Differential Equations and Quasiconformal Mappings in the Plane*, Princeton Mathematical Series, **48** (2009)

[4] K. Astala, J. L. Mueller, A. Perämäki, L. Päivärinta, and S. Siltanen, *Direct electrical impedance tomography for nonsmooth conductivities*, Inverse Problems and Imaging, **5**, 531-549 (2011).

[5] A. Bjŏrck, *Numerical methods for least squares problems*, Siam, 1996.

[6] P. Daripa, *A fast algorithm to solve nonhomogeneous Cauchy-Riemann equations in the complex plane*, SIAM J. Sci. Statist. Comput., **13**, 1418-1432 (1992).

[7] P. Daripa, *A fast algorithm to solve the Beltrami equation with applications to quasiconformal mappings*, J. Comput. Phys., **106**, 355-365 (1993).

[8] P. Daripa and D. Mashat, *An efficient and novel numerical method for quasiconformal domains*, Numer. Algorithms, **18**, 159-175 (1998).

[9] P. Daripa, *On applications of a complex variable method in compressible flows*, J. Comput. Phys., **88**, 337-361 (1990).

[10] T. K. DeLillo, *The accuracy of numerical conformal mapping methods: a survey of examples and results*, SIAM J. Numer. Anal., **31**, 788-812 (1994).

[11] T. A. Driscoll and L. N. Trefethen, *Schwarz-Christoffel mapping*, Cambridge Monographs on Applied and Computational Mathematics **8**, Cambridge University Press, Cambridge (2002).

[12] D. Gaidashev, D. Khmelev, *On numerical algorithms for the solution of a Beltrami equation*, SIAM J. Numer. Anal. **46**:5 (2008) 2238–2253.

[13] F. P. Gardiner, N. Lakic, *Quasiconformal Teichmüller theory*, Math. Surv. Monogr. 76, Am. Math. Soc., Providence, RI (2000)

[14] X. D. Gu, W. Zeng, F. Luo, and Sh-T. Yau, *Numerical computation of surface conformal mappings*, Comput. Methods Funct. Theory, **11**, 747-787(2011).

[15] Zh.-X. He, *Solving Beltrami equations by circle packing*, Trans. Amer. Math. Soc. **322**, 657-670 (1990).

[16] P. Henrici, *Applied and Computational Complex Analysis*, vol. **3**, Wiley, New York (1986).

[17] Y. Imayoshi and M. Taniguchi *An introduction to Teichmüller space*, Springer-Verlag, Tokyo, 1992.

[18] P. K. Kythe, *Computational conformal mapping*, Birkhäuse, Boston (1998).

[19] O. Lehto, *Univalent Functions and Teichmüller Spaces*, Springer-Verlag, New York (1995).

[20] O. Lehto and K. I. Virtanen, *Quasiconformal mappings in the plane* , 2nd ed., Springer-Verlag, New York-Heidelberg, 1973.

[21] B. Lévy, S. Petitjean, N. Ray and J. Maillot, *Least Squares Conformal Maps for Automatic Texture Atlas Generation*, *ACM Transactions on*

Graphics (TOG), Proceedings of ACM SIGGRAPH 2002 **21**:362–371 (2002).

[22] L. M. Lui, K. C. Lam, T. W. Wong, and X. Gu, *Texture Map and Video Compression Using Beltrami Representation*, SIAM J. Imaging Sci. **6**:1880–1902 (2013).

[23] L. M. Lui, T. W. Wong, P. M. Thompson, T. F. Chan, X. Gu, and S. T. Yau, *Compression of surface registrations using Beltrami coefficient*, IEEE CVPR, 2010.

[24] L. M. Lui, K. C. Lam, S-T. Yau, and X. Gu, *Teichmüller extremal mapping and its applications to landmark matching registration*, `arXiv:1211.2569v1`.

[25] C. B. Morrey, *On the solutions of quasilinear elliptic partial differential equations*, Trans. Amer. Math. Soc., **43**, 126-166 (1938).

[26] C. W. Mastin and J. F. Thompson, *Discrete quasiconformal mappings*, Z. Angew. Math. Phys., 29, 1-11, (1978).

[27] C. Mastinan and D. J. Thompson, *Quasiconformal mappings and grid-generation*, SIAMJ. Sci. Statist. Comput., **5**, 2, 305-310, (1984).

[28] S. Morosawa, Y. Nishimura, M. Taniguchi and T. Ueda, *Holomorphic dynamics*, Cambridge Univ. Press, Cambridge, 2000.

[29] J. R. Munkres, *Elementary Differential Topology. Lectures given at Massachusetts Institute of Technology, Fall, 1961.* Revised edition. Annals of Mathematics Studies, No. 54 Princeton University Press, Princeton, N.J.

[30] Ch. Pommerenke, *Boundary behavior of conformal maps*, Springer-Verlag, New York, 1992.

[31] R. M. Porter, *History and recent developments in techniques for numerical conformal mapping*, Proceedings of the International Workshop on Quasiconformal Mappings and Their Applications (IWQCMA05), 2005.

[32] R. M. Porter and H. Shimauchi, *Numerical solution of the Beltrami equation via a purely linear system*, arXiv:1405.7359.

[33] B. Rodin and D. Sullivan, *The convergence of circle packings to the Riemann mapping*, J. Differential Geom., **26**-2, 349-360 (1987).

[34] K. Stephenson, *Introduction to circle packing. The theory of discrete analytic functions*, Cambridge University Press, Cambridge (2005)

[35] T. Sugawa, *An application of the Loewner theory to trivial Beltrami coefficients*, in preparation.

[36] G. Szegö, *Conformal mapping of the interior of an ellipse onto a circle*, American Mathematical Monthly **57**:474–479 (1950).

[37] M. Trott, *The Mathematica GuideBook for Numerics*, Springer, New york. (2006).

[38] J. Weisel, *Numerische ermittlung quasikonformer abbildungen mit finiten elementen*, Numer. Math., **35**, 201-222, (1980).

[39] G. B. Williams, *A circle packing measurable Riemann mapping theorem*, Proc. Amer. Math. Soc. **134**, 2139-2146, (2006).

[40] E. T. Whittaker and G. N. Watson, *Course of Modern Analysis*, reprint of the fourth (1927) edition, Cambridge Mathematical Library, Cambridge University Press, Cambridge (1996).

[41] Wolfram Research, Inc., *Mathematica*, Version 10.0, Champaign, IL (2014).